Julius-Maximilians-Universität Würzburg
Graduate School of Life Sciences
Section: Biomedicine

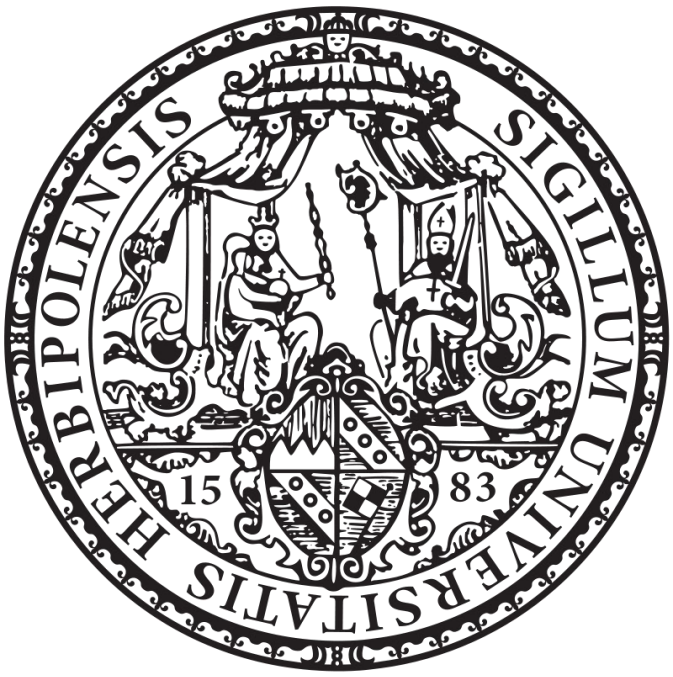


# Development of anti-TNF antibody-gold nanoparticles (anti-TNF-AuNPs)

## Entwicklung von Anti-TNF-Antikörper-Gold-Nanopartikeln

**Doctoral thesis for a doctoral degree**

submitted by

**Ahmed Aido**

from Aleppo

Würzburg, 2023

**Submitted on:** ……

**Members of the promotion committee:**

**Chairperson:** Prof. Dr. Thomas Dandekar

**Primary Supervisor:** Prof. Dr. Harald Wajant

**Second Supervisor:** Prof. Dr. Andreas Beilhack

**Third Supervisor:** Prof. Dr. Thomas Müller

**Date of Public Defence: ……..……**

**Date of Receipt of Certificates: ……..**

# Eidesstattliche Erklärung

Hiermit erkläre ich an Eides statt, die Dissertation “Entwicklung von Anti-TNF-Antikörper-Gold-Nanopartikeln“ eigenständig, d.h. insbesondere selbständig und ohne Hilfe eines kommerziellen Promotionsberaters, angefertigt und keine anderen als die von mir angegebenen Quellen und Hilfsmittel verwendet zu haben.

Ich erkläre außerdem, dass die Dissertation weder in gleicher noch in ähnlicher Form bereits in einem anderen Prüfungsverfahren vorgelegen hat.

Würzburg, den

Unterschrift
(Vor- und Zuname)

# Affidavit

I hereby confirm that my thesis entitled “Development of anti-TNF antibody-gold nanoparticles (anti-TNF-AuNPs)” is the result of my own work. I did not receive any help or support from commercial consultants. All sources and / or materials applied are listed and specified in the thesis.

Furthermore, I confirm that this thesis has not yet been submitted as part of another examination process neither in identical nor in similar form.

Würzburg,
Date

Signature

# Correction of the Figure 9 legend

**Figure 9: DLS size distributions of colloidal AuNPs.**

UnPEGylated (left) AuNPs and AuNPs after PEGylation with carboxyl-PEG-SH (center) and mPEG-SH (right). Three reads were performed using the DLS device, and the SD of the results were as follows: AuNPs unPEGylated (0 nm), after PEGylation with carboxyl-PEG-SH (3.5 nm) and mPEG-SH (3.2 nm).

This work was achieved in the period from **05. November 2019** till **31. December 2022** in the Division of Molecular Internal Medicine, University Hospital of Würzburg under the supervision of **Prof. Dr. Harald Wajant.**

## Acknowledgements

I would like to express my sincere gratitude to my advisor **Prof. Dr. Harald Wajant** for the infinite support of my scientific journey during the last four years, for his patience, motivation, and massive knowledge; and for providing me with the opportunity to work in such a supportive and collaborative research environment. He guided me always toward the right direction whenever he thought I needed it. Furthermore, I would like to thank the other members of my promotion committee, the second and the third supervisors, Prof. Dr. Andreas Beilhack and Prof. Dr. Thomas Müller.

It is my pleasure to express my heartfelt thanks to my brother and friend Dr. Mohamed Anany for his supporting and standing along the total period of my work in the lab, for his delivering me the basic techniques and for his priceless comments on this thesis. My thanks go also to Dr. Abdelaziz Elgaml, Dr. Olena Zaitseva and Dr. Isabell Lang for their support and the helpful scientific discussion. Their invaluable expertise contributed to the success of my research. Moreover, I would like to express my sincere gratitude to the technical team in the lab, special mention here Mrs. Daniela Weisenberger who have been instrumental in the successful completion of my PhD project. Without their support and dedication, this project would not have been possible. I would also like to acknowledge all my other colleagues for their cooperation and the motivating working environment they achieved in the lab. The gratitude goes also to the scientists and engineers in the Department for Functional Materials in Medicine and Dentistry (FMZ) in Würzburg, in particular, Mrs. Friederike Kaiser and Mr. Philipp Stahlhut for their time and efforts by performing the ICP-MS measurement and taking the STEM images of gold nanoparticles.

I extend my heartfelt thanks to InoCure team in Prague, in particular, Dr. Aiva Simaite and Mr. Matej Buzgo who provided invaluable assistance with experimental design, data collection, and analysis. Their knowledge and expertise have been indispensable in overcoming the technical challenges I encountered during this project. Thanks to the challenging and beautiful days and nights I spent in InoCure, where the first station of my research was, this achievement sees the light of day.

I am also grateful to the administrative and scientific staff and colleagues of the I-DireCT consortium, a project of Marie Curie Innovative Training Network (ITN) within the H2020 Programme, who have operated the activities and participated in the internal meeting efficiently and accurately. Their contributions have played a crucial role in my research.

Finally, I would like to express the deepest thanks and gratitude to my **God** for pushing and orienting me to reach this goal and ambition. My very profound gratitude should be expressed to my parents, my parents in law and to my lovely wife Bayan for providing me with unfailing support and continuous encouragement throughout my years of study and life, through the nights and days of researching and writing this thesis. Nobody has been more important to me in the pursuit of this achievement than the

members of my family: my father Mr. Ziad, my mother Mrs. Sousn, my second father Dr. Anwar and my second mother Dr. Mayada, whose love and guidance are with me in whatever I pursue.

Last but not least, the sweetest and sincere feelings of love go to my supportive wife and partner in the long journey in science and life, Bayan, and my wonderful little children Ziaddin & Najmedin who provided and are still giving unending inspiration. Thank you for being an integral part of this journey, and for making my PhD project a memorable and rewarding experience.

*Ahmed Aido*

*Dedicated to*

*my beloved mother* ***Sousn,***

*my lovely wife* ***Bayan***

*and my sweetheart children* ***Ziaddin*** *&* ***Najmedin.***

## Table of Contents

# 1. Introduction

## 1.1. The Biomedical Applications of Gold Nanoparticles and Bioinks

### 1.1.1. Gold Nanoparticles

Gold nanoparticles (AuNPs) are tiny particles of gold which are termed nanoparticles because of their diameter of 1 to 100 nm. Their dispersion in water is known as colloidal gold. Gold nanoparticles can be synthesized via variety of routes, Turkevich introduced in 1952 a method which is recognized to be one of the earliest works to produce AuNPs using the reduction reaction of gold ions, chloroauric acid ($HAuCl_4$), by citrate at 100°C (Turkevich, Stevenson and Hillier, 1951). This method was later optimized by Frens in the 1972 for more control of the produced particle size (FRENS, 1973).

Different morphology of AuNPs can be obtained, however, the spherical and rod-shaped AuNPs are considered to be the most common used shapes in the biomedical applications, which can be due to the optical features that these shapes possess (Kim *et al.*, 2015). The difference in shape and size might account also to differences in their optical properties and cellular uptakes which leads to increase the wide use of AuNPs in the current biomedical applications (Moustakas *et al.*, 2022).

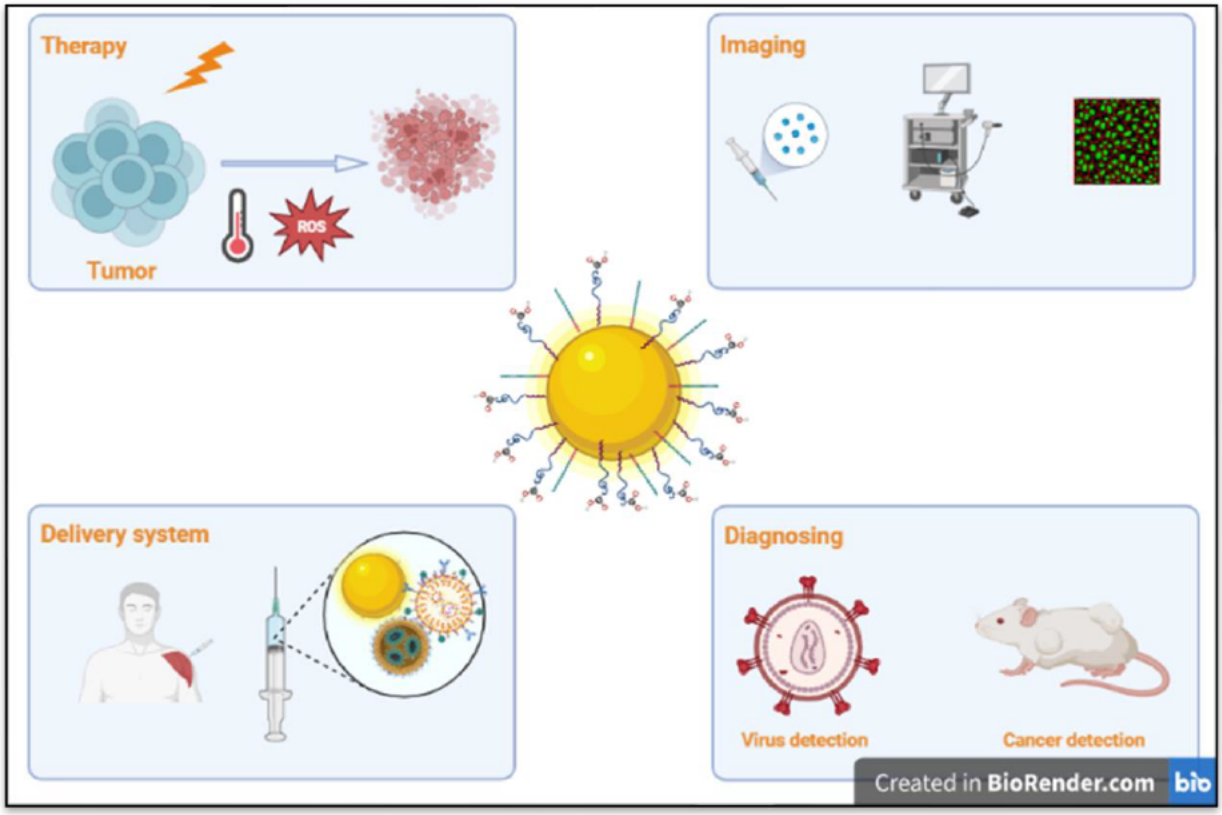


**Figure 1: Graphical illustration of the diverse applications of gold nanoparticles**:

They encompass fields of therapy, imaging, detection, diagnostics, and precise drug delivery , pictures were created in Biorender.com according to the reference (Moustakas *et al.*, 2022).

Gold in addition to silver nanoparticles are recognized to be the most attractive inorganic metallic particles according to their special physical and chemical properties. Moreover, the dispersion of gold nanoparticles is known to create a stable colloidal which can be even re-covered by re-dispersion and ultracentrifugation processes. The physicochemical and optoe-lectronic properties of the spherical AuNPs such as surface plasmon resonance, conductivity, good surface-to-volume ratio allow their application in different biomedical fields (Moustakas *et al.*, 2022), (**Figure 1**). Additionally, the excellent biocompatibility, and low toxicity of gold nanoparticles extend the possibilities to exploit them as drug delivery systems (Dzimitrowicz *et al.*, 2019). Gold nanoparticles (AuNPs) are thus widely used for different biomedical appli-cations including the use as a platform for nano-biological conjugates, that can be easily modified and decorated with various types of molecules such as oligonucleotides (Zhang *et al.*, 2011), antibodies (El-Sayed, Huang and El-Sayed, 2005), and proteins (You, Arvizo and Rotello, 2006). All these properties combined make gold nanoparticles a promising tool to deliver the therapeutic agents to the targeted cells.

### 1.1.2. Bioink and Biofabrication

The integration of modern technologies in development of biomaterials has been expanded recently. The main purpose of these technologies was to improve the field of artificial biological tissue engineering (Langer and Vacanti, 1993; Khademhosseini and Langer, 2016). Bioprinting is basically an automated fabrication of 3D cell-containing constructs, these are built via layer-by-layer procedures upon the deposition of biomaterials in a precise spatial arrangement under the commanding of specific related algorithm and computer aid design (CAD) (**Figure 2**). The goals of this approach encompass two basic areas: (I) tissue engineering and regenerative medicine (TERM) for the purposes of tissue repairment, regeneration and replacement; and (II) creation of 3D *in vitro* models for disease mechanism´s study and drug´s screening (Pati, Gantelius and Svahn, 2016). Furthermore, the developed 3D bioprinting methods allow fabrication of highly complex constructs, which consist of combination of cells and biocompatible materials or bioinks, basically hydrogels, such as methacrylate-modified gelatin (GelMA), enriched with molecules, necessary for cells´ differentiation and functionality, which include amongst other growth factors (Schloss, Williams and Regan, 2016; Zhang *et al.*, 2016). These constructs are distinct from the conventional prefabricated scaffolds for cell loading (Pati, Gantelius and Svahn, 2016), that the mixing with live cells eases the ability to build microstructures between the cells leading to mimic the natural networking and the distribution of cells in the native tissues. It is noteworthy to mention, that the term “bioink” refers to the printing materials when they are mixed with live cells (Moroni *et al.*, 2018). In addition, the incorporation of nanoparticles in 3D

printed constructs has highlighted promising properties to stimulate the printed cells sustainably, in addition to medical imaging applications (Li *et al.*, 2020, 2022).

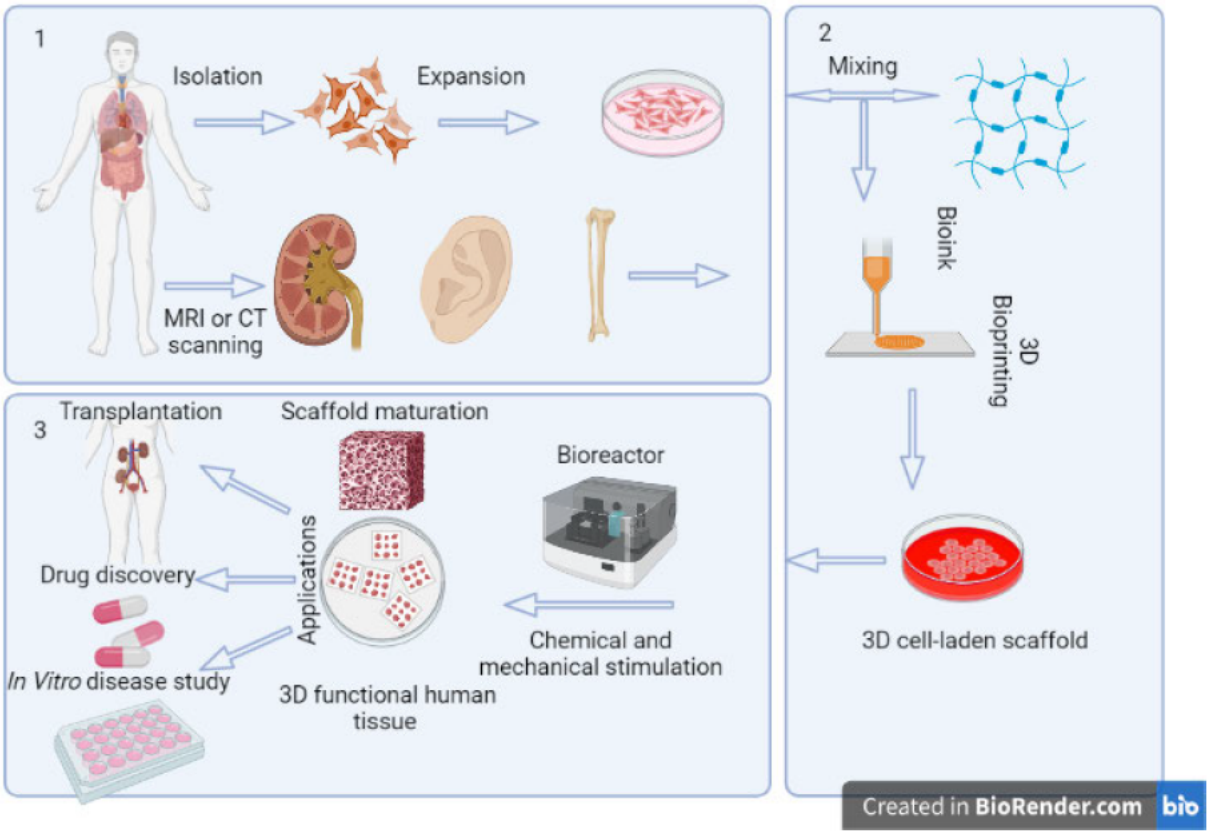


**Figure 2**: **The steps of 3D bioprinting of human tissues**.

(1) In pre-processing: cell preparation , Magnetic resonance imaging (MRI) or Computed tomography (CT) scanning to collect the structural information and to create the printing model, such as ear, kidney, and bone; (2) In processing: bioink preparation, 3D bioprinting of 3D cell-laden scaffolds guided by the MRI or CT scanning tissue models; (3) In post-processing: bioreactor culture system for *in vitro* scaffold maturation to build the 3D functional human tissues, and potential applications of the 3D bioprinted human tissues, pictures were created in Biorender.com according to the reference (Zhang *et al.*, 2016) .

Moreover, the integrated nanoparticles can play a critical role in the regulation of the grow and differentiation processes of the embedded cells via the immobilized molecules on the surface of the particles (Fathi-Achachelouei *et al.*, 2019; Zhang *et al.*, 2023). In the perspective of these outstanding benefits of the AuNPs-embedded bioink, new approaches can be investigated to fabricate novel local stimulatory or inhibitory systems.

### 1.2. TNF Receptor Superfamily (TNFRSF)

TNF receptor superfamily (TNFRSF) receptors, also named tumor necrosis factor receptors (TNFRs), are a family of proteins that play a crucial role in the orchestrating of immune and inflammatory responses in the body (Parameswaran and Patial, 2010). They are found on the surface of cells that play a crucial role in the regulation of the immune system. These receptors are responsible for recognizing and responding to the binding of ligands of the tumor necrosis factor superfamily (TNFSF). TNF receptors play a key role the activation of immune cells and the release of pro-inflammatory cytokines. Additionally, they are involved in various physiological and pathological processes, such as cell survival, tumorigenesis, autoimmunity, and tissue repair. Thus, the interaction with their ligands regulates innate and adaptive immune responses, among others by natural killer cell activation, T cell co-stimulation and B cell homeostasis and activation (Bodmer *et al.*, 2002). Understanding the function and regulation of TNF receptors is important for developing of effective treatments for a wide range of diseases, including cancer, autoimmune disorders, and inflammatory conditions (Mehta, Gracias and Croft, 2018).

There are 29 TNFRs in humans, mostly type I transmembrane proteins, which consist of an extracellular N-terminal domain and an intracellular C-terminal domain (Craig Smith and Farmh, 1994; Ashkenazi and Dixit, 1998; Wallach *et al.*, 1999; Idriss and Naismith, 2000). They are expressed on the surface of numerous cells that play a crucial role in the regulation of the immune system including among other B lymphocytes and monocytes and antigen presenting cells (APC) such as macrophages, dendritic cells but also by a variety of non-immune cells such as endothelial cells and fibroblasts. Additionally, some TNF receptors, such as CD40 and 41BB, are highly expressed on various malignant cells (Tsai *et al.*, 1996; Falvo, Tsytsykova and Goldfeld, 2010; Sedger and McDermott, 2014).

The TNFRs are characterized by the presence of cysteine-rich domains (CRDs) in the extracellular domains (**Figure 3**). The CRDs basically contain six cysteine residues involved in the formation of three disulfide bonds. The number of CRDs included in the TNF receptors varies from one to four (Bodmer *et al.*, 2002; Macewan, 2002; Dostert *et al.*, 2019). It has been shown that oligomerization of TNFRSF receptors in a ligand-independent fashion is caused by the first N-terminal CRD which has been accordingly be termed as pre-ligand association domain (PLAD) (Chan *et al.*, 2000; Bodmer *et al.*, 2002).

Noteworthy, the diversity of intracellular domains found in the TNFRSF receptors leads to different signaling pathways triggered by the various receptors of this superfamily (Beutler and Bazzoni, 1998; Idriss and Naismith, 2000). Depending on structural and functional homologies, TNFRs could be categorized into three subgroups: (I) Death receptors (DRs), for example in TNFR1 and FAS (CD95), possess in their cytoplasmic part a domain containing

around 80 amino acids called death domain (DD). This domain exists also in some other DR-associating proteins which can initiate cell death signaling pathways, such as TNF receptor type 1-associated death domain protein (TRADD) and FAS associated death domain (FADD) (Tartaglia *et al.*, 1993; Hsu, Xiong and Goeddel, 1995; Pobezinskaya and Liu, 2012). Silencer of death domain (SODD) is also one type of those associating proteins which contains also a death domain, but it competes with the other DD-interacting proteins in binding with DD in TNFRs, the engagement between these death domains leads to the formation of a complex which initiates caspase recruitment and activation and ultimately induction of apoptosis (Jiang *et al.*, 1999; Sessler *et al.*, 2013; Dostert *et al.*, 2019). (II) Non-death receptors or TRAF-interacting receptors which lack a DD but contain one to three binding motifs for adapter proteins of the TNF receptor associated factor (TRAF) family which is involved in inducing proinflammatory signaling pathways, additionally, non-death receptors are implicated in cell survival, proliferation, and cytokine production, examples of these receptors are among other CD40, 41BB and lymphotoxin β receptor (LTβR) (Dostert *et al.*, 2019). (III) Decoy receptors, such as TRAILR3 (also known as DcR1), TRAILR4 (also known as DcR2), DcR3 and osteoprotegrin (OPG), are soluble or membrane-bound TNF receptors which lack the cytoplasmic signaling domain or possess a truncated one. It is thought that these receptors involved in regulation of the activity of other TNFRs. Noteworthy, the specificity of death receptors to recruit a caspase activating complex to trigger cell death could be converted to trigger proinflammatory pathways (Wajant, Henkler and Scheurich, 2001; Macewan, 2002; Wajant, 2015) (**Table 1**).

### 1.2.1. Fn14 receptor

Fibroblast growth factor inducible 14 (Fn14) is a member of the TNFRSF of 129 amino acids (Meighan-Mantha *et al.*, 1999; Wiley *et al.*, 2001). . It has been found that Fn14 is frequently expressed in solid tumors (Feng *et al.*, 2000; Willis *et al.*, 2008) and in tissue injury, moreover, its activation might be involved with cancer, chronic autoimmune diseases and acute ischaemic stroke (Winkles, 2008; Wajant, 2013). The Fn14 cytoplasmic tail, only comprising 28 amino acids, does not contain a death domain, instead, it contains a single TNFR-associated factor (TRAF) binding motif. The extracellular cysteine rich domain (CRD) of Fn14 can exclusively bind TNF-like weak inducer of apoptosis (TWEAK), which is a member of the TNFSF. Fn14 and TWEAK regulate a variety of cellular activities, such as proliferation, migration, differentiation, and inflammation (Winkles, 2008). Noteworthy, the triggering of Fn14 leads to activation of the classical and alternative nuclear factor-κB (NF-κB) signaling pathways in addition to the enhancement of TNF-induced cell death (Saitoh *et al.*, 2003; Wajant, 2013)

### 1.2.2. CD40 receptor

CD40 is also a member of the TNFRSF, which regulates immune activation and mediates tumor apoptosis. It is expressed by antigen-presenting cells (APC) including dendritic cells and B cells. The ligation of CD40 receptor with its corresponding ligand (CD40L), which is expressed on T cells and other non-immune cells, leads to the expression of MHC and costimulatory molecules such as CD86, induces the production of pro-inflammatory cytokines such as IL-12, and induces T cell activation which is essential to the immune responses (Elgueta *et al.*, 2009). Additionally, CD40 is also expressed on many tumor cells and its ligation mediates a direct cytotoxic effect, thus, CD40 is considered as a very critical target in harnessing anti-tumor immunity.

### 1.2.3. 4-1BB receptor

4-1BB (known as CD137 or TNFRSF9, encoded byTNFRSF9) again belongs to the TNFRs, which is among other one of the multiple T cell co-stimulatory receptors such as CD40 and is recognized as T cell- and non-T cells activating molecule which play roles also in expansion, acquisition of effector function, survival, and development of T cell memory. 4-1BB is expressed on a variety of non-T cells including activated dendritic cells (DCs), monocytes, neutrophils, B cells and natural killer (NK) cells, and promotes their individual effector functions. The T cell- and non-T cell-activating ability of 4-1BB is the basis of its powerful anti-cancer function. Additionally, 4-1BB is included in generating immunological memory and sustaining T cell immune responses (Vinay and Kwon, 2011). Moreover, the induction of 4-1BB leads to the activation, among other, of NF-κB and MAPK pathways through TRAF1 and TRAF2, which mediate to expression of survival genes and decrease the expression of pro-apoptotic Bim (Mbanwi and Watts, 2014).

### 1.2.4. TNFR2

The ligand TNFα (TNFSF1B), a type II transmembrane protein and the secreted ligand Lymphotoxin-α (LTα, TNFSF1A) can bind TNFRII (Etemadi *et al.*, 2013). It has been reported that in contrast to TNFR1, which is expressed on almost all mammalian cell types, TNFR2 is expressed particularly on immune cells and some other cell types such endothelial cells, neural cells, and Mesenchymal Stem Cells (MSCs) and its stimulation with TNFα leads to cell survival and proliferation (Yan, Zheng and Xu, 2018; Yang *et al.*, 2018; Naserian *et al.*, 2020). Whereas both TNFR1 and TNFR2 share the structure of the extracellular domain of 4 cysteine rich domains, TNFR2, unlike TNFR1, lacks death domain (DD) in its cytoplasmic tail, that hinders consequently its ability to directly activate the apoptotic cascade through DD adaptors (Aggarwal, 2003). Upon the ligation of TNFR2 with TNFα, TNFR-associated factor 1

(TRAF1) and TRAF2 are recruited, which leads to NF-κB activation promoting cell survival (Siegmund, Wagner and Wajant, 2022).

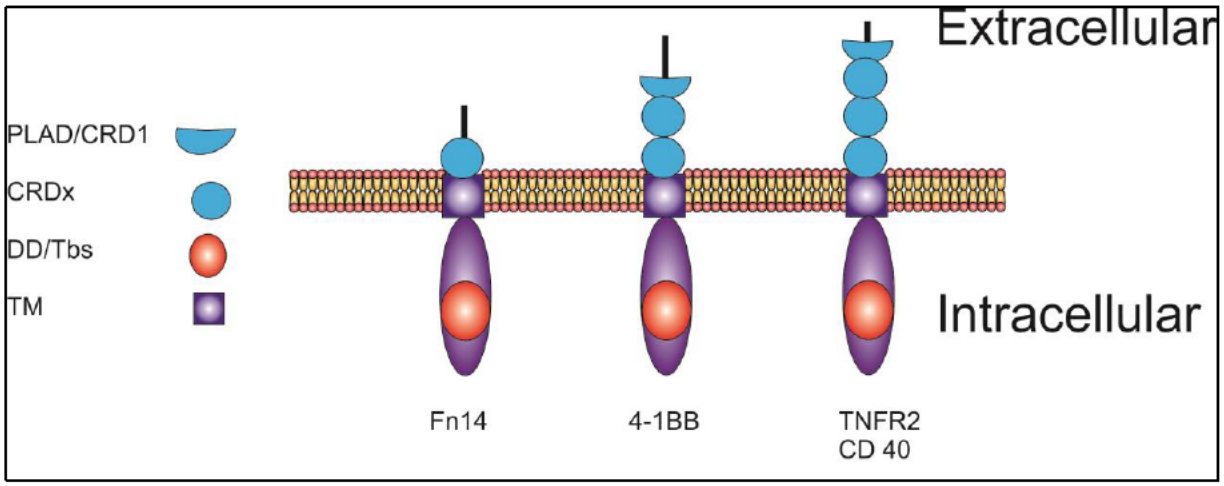


**Figure 3: Domain architecture of TNF receptors.**

Some types of TNFRSF receptors, which are characterized by having one or more cysteine-rich domains (CRDs) in their extracellular parts. TNFRs which are categorized as death receptors contain in their intracellular domain the death domain (DD), such as TNFR1 of CD95. Hear we showed the structure of TRAF-interacting receptors which lack the death domain but possess instead TRAF binding sites (TBS). TM reveals to the transmembrane region of the receptor.

**Table 1: TNFRSF receptors, the corresponding ligands, and their intracellular binding partners**

| TNFRSF receptor (TNFRSF#, other names) | TNFSF ligand (TNFSF#, other names) | Intracellular binding partner |
|---|---|---|
| **I) Death Receptors** | | |
| TNFR1(1a, CD120a) | TNF (2, TNFα), LTα (1, TNF-β), LTβ (3) | TRADD, FADD, RIP |
| Fas (6, CD95) | FasL (6, CD178) | FADD |
| TRAILR1 (10A, DR4, CD261) | TRAIL/Apo2L (10, CD253) | FADD, TRADD, RIP |
| TRAILR2 (10B, DR5, CD262) | TRAIL/Apo2L (10, CD253) | FADD, TRADD, RIP |
| NGFR (16, p75NTR, CD271) | NGF (not a TNFSF member) | NADE |
| DR3 TL1A (15, VEGI) | (25 or 12, TRAMP), TWEAK (12) | TRADD, FADD |
| DR6 (21, CD358) | N-APP (not a TNFSF member) | TRADD, RIP |
| EDAR | EDA-A1 | EDARADD |
| **II) TRAF-interacting Receptors** | | |
| TNFR2 (1b, CD120b) | TNF (2, TNF-α), LTα (1, TNF-β), LTβ (3) | TRAF1–3 |
| LTβR (3) | LTβ (3), LTαβ2 | TRAF2, TRAF3, TRAF5 |
| OX40 (4, CD134) | OX40L (4, CD252) | TRAF1–3, TRAF5, TRAF6 |
| CD40 (5) | CD40L (5, CD154) | TRAF1–3, TRAF5, TRAF6 |
| CD27 (7) | CD27L (7, CD70) | TRAF2, TRAF3, TRAF5 |
| CD30 (8) | CD30L (8, CD153) | TRAF1–3, TRAF5 |
| 4-1BB (9, CD137) | 4-1BBL (9, CD137L) | TRAF1–3 |
| RANK (11A, CD265) | RANKL (11, TRANCE, D254) | TRAF1–3, TRAF5, TRAF6 |
| Fn1 (12A, TWEAKR; CD266) | TWEAK (12) | TRAF2, TRAF6 |
| TACI (13B, CD267) | APRIL (13, CD256) | TRAF2–3, TRAF5, TRAF6 |
| BAFFR (13C, BR3, CD268) | BAFF (13B/20, BLys, THANK, CD257) | TRAF2, TRAF3, TRAF6 |
| HVEM (14, CD270) | LIGHT (14, CD258), LTα (1, TNF-β) | TRAF1–3, TRAF5 |
| BCMA (17, CD269) | APRIL (13, CD256), BAFF (13B/20, BLys, THANK, CD257) | TRAF1–3, TRAF5, TRAF6 |
| GITR (18, AITR, CD357) | GITRL (18, AITRL, TL6) | TRAF1–5 |
| TROY (19, TAJ) | ? | TRAF2, TRAF5, TRAF6 |
| RELT (19L) | ? | TRAF1 |
| XEDAR (27) | EDA-A2 | EDA-A2 |
| **III) Decoy receptors** | | |
| TRAILR3 (10C, DcR1, D263) | TRAIL/Apo2L (10, CD253) | n/a |
| TRAILR4 (10D, DcR2, D264) | TRAIL/Apo2L (10, CD253) | n/a |
| OPG (11B) | TRAIL/Apo2L (10, CD253), RANKL (11, TRANCE, CD254) | n/a |
| DcR3 (6B) | FasL (6), TL1A (15, VEGI), LIGHT (14, CD258) | n/a |

## 1.3. TNFSF Ligands

It has been reported that two proteins produced from macrophages and lymphocytes, called lymphotoxin (LT) and tumor necrosis factor (TNF) lead to the lysis of some types of cells (e.g. tumor cells), these molecules were considered as members of wide group of structurally related proteins which constitute a ligand superfamily, this group has been termed as tumor necrosis factor superfamily (TNFSF) (Carswell *et al.*, 1975). The name tumor necrosis factor was derived from the observation of rapid necrotic regression of certain forms of tumors caused by these proteins after submission to a bacterial antigen (Carswell *et al.*, 1975). These proteins are trimeric transmembrane proteins from which soluble ligand trimers can be released via proteolytic processing (Carswell *et al.*, 1975).

TNF is a signaling molecule produced by various cells in response to infections, inflammation, and other stimuli. Moreover, TNF is a key mediator of the immune response and has a crucial role in orchestrating and activation of immune cells, and the release of proinflammatory cytokines. TNF plays a dual role in the body, as it can either trigger inflammation to fight infections or cause tissue damage if its levels are excessive or prolonged. A variety of diseases, such as cancer, autoimmune disorders (e.g., rheumatoid arthritis, psoriasis, inflammatory bowel disease), and inflammatory conditions can be consequences of the imbalance between TNF production and its removal from the body. Based on that, TNF has been considered as an attractive therapeutic target for the treatment of these diseases, that blocking its action can help to reduce inflammation and tissue damage. TNFSF ligands share common distinctive hallmark, the "TNF homology domain" (THD), this highly conserved motif exists in the extracellular C-terminus of the ligands and plays a crucial role for binding to the cysteine-rich domains (CRDs) of TNF receptors and the formation of trimeric molecules (Fesik, 2000; Idriss and Naismith, 2000; Bodmer *et al.*, 2002; Hehlgans and Pfeffer, 2005) (**Figure 4**). The homology of 20–30% amino acid in their interacting protein interfaces leads to the assembly of the trimeric tertiary structure (**Figure 5**). TNFSF ligands are type II trans-membrane proteins consisting of intracellular N-terminus and extracellular C-terminus. These ligands can be released from the cell membrane by proteolytic cleavage mediated by metalloproteinases. Moreover, some TNFSF ligands are naturally expressed as soluble molecules, e.g., LTα. Although the ability of the soluble and the membrane-bound TNFSF ligands to bind to their respective receptors, they differ in their potency. It is worth mentioning that a wide group of TNFRs are not responding to soluble ligand trimers, however, these receptors become properly activated by the membrane-bound ligand forms or soluble ligand molecules when bound to the cell surface, e.g., via chemical means or genetic fusion with an anchoring domain recognizing a membrane-associated target (Wyzgol *et al.*, 2009; Wajant, 2015). For example, while the soluble and the transmembrane variant of TNF can both activate strongly TNFR1, TNFR2 is efficiently

activated only by the membrane-bound TNF form (Grell *et al.*, 1995). Another example of the variety of the signal transduction mode of soluble and membrane-bound TNF ligands is the TNF-like weak inducer of apoptosis (TWEAK), which plays a dual role in the activation of the classical and noncanonical NF-κB pathway (Brown *et al.*, 2003; Saitoh *et al.*, 2003; Roos *et al.*, 2010). Although both soluble and membrane TWEAK interact with Fn14 receptor, they differ with respect to the activation of the two NF-kB pathways. Whereas both TWEAK variants are potent inducers of TNFR-associated factor-2 depletion, NF-kB–inducing kinase accumulation and p100 processing, hallmarks of activation of the noncanonical NF-kB pathway, in addition to the enhancement of TNF-induced cell death, only the membrane-anchored variant of TWEAK can trigger the classical NF-kB signaling pathway strongly. Like other soluble TNF ligands with a poor capability to activate their corresponding receptors, sTWEAK acquires an activity resembling those of the transmembrane ligand by oligomerization or cell surface-immobilization. Blocking Fn14 receptor leads to the inhibition of NF-kB signaling regardless of the TWEAK form used for stimulation, which indicates that the differential activities of the two TWEAK variants on classical and noncanonical NF-kB signaling are not related to the triggering of different receptors (Roos *et al.*, 2010).

Similarly, It has been demonstrated that the inactive soluble variant of 41BBL can become highly active and mimic their related transmembrane form via immobilizing with the FAP-positive cells upon the fusion with sc40, an Ab fragment recognizing the cell surface Ag FAP, resulting in a 1000-fold increase in activity by eliciting a strong Induction of interleukin-8 production, a hallmark of classical NF-kB signaling pathway (Wyzgol *et al.*, 2009). Last but not least, although both forms of CD40L ligands, the transmembrane and the soluble, display strong ability to stimulate their related receptor(s) via activating the canonical NF-kB signaling pathway, the binding of fusion protein of CD40L to FAP still enhanced its activity, which can be shown by shifting the ED50 value of the construct to an 25-fold lower concentration (Wyzgol *et al.*, 2009).

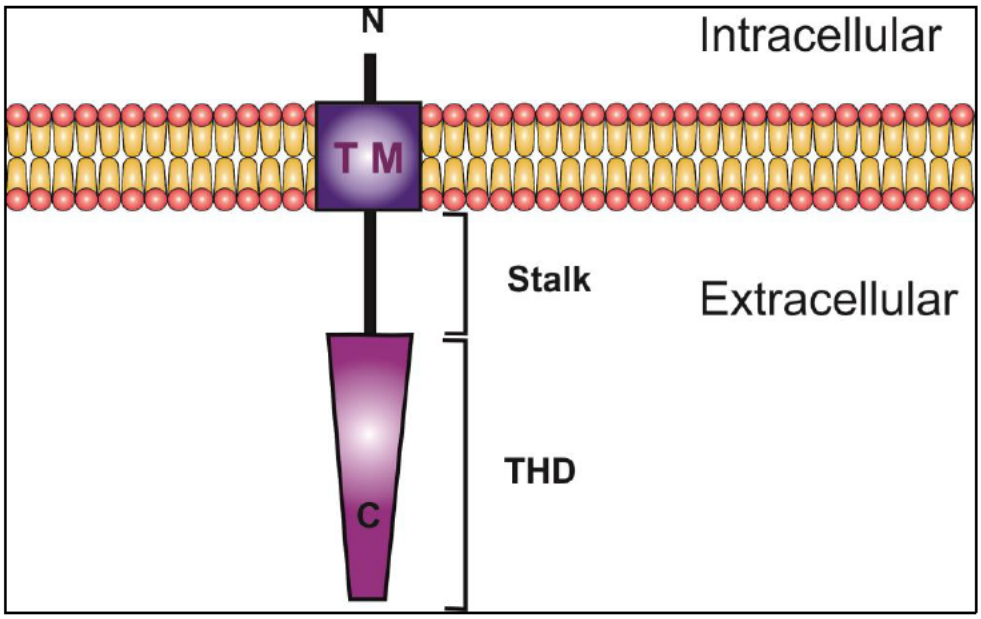


**Figure 4: Domain architecture of the membrane TNF ligand.**

The THD domain which are responsible for the interacting with CRDs of TNF can be cleaved throug the stalk region to act as soluble TNF ligand.

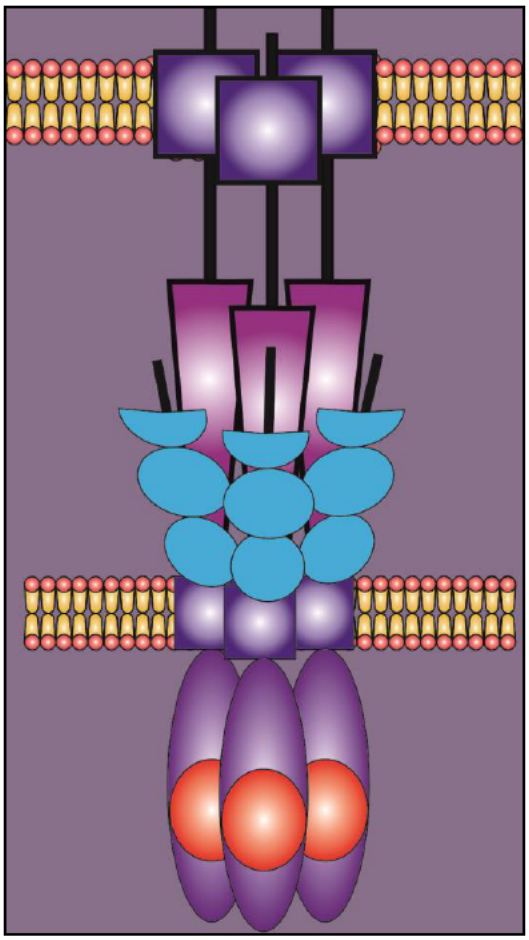

**Figure 5: Schematic representation of TNF ligands/receptors interaction.**

Membrane TNF ligands, such as CD40 ligand interact as homotrimeric protein that can bind to their cognate receptors as a trimer, but can also form higher-order structures, such as hexamers and larger multimers, which can induce more potent signaling through CD40

## 1.4. Innate and adaptive Immunity and the ways of Immunotherapy to treat the Cancer

There is strong evidence that a successful immune response to eliminate cancer is built upon the coordination between the innate and adaptive arms of the immune system. The innate immune cells, including natural killer cells (NK), dendritic cells (DC), macrophages, myeloid-derived suppressor cells (MDSCs), and innate lymphoid cells (ILCs), play a crucial role in altering the tumor microenvironment (TME) and modulating the adaptive tumor response. It has been shown that adaptive immune cells, such as B lymphocytes, CD4+ helper T lymphocytes, and CD8+ cytotoxic T-lymphocytes (CTLs), are the most effective cells to eliminate tumors. Thus, the understanding of the interaction between these two arms of the immune system at the molecular level will allow to potentiate the immune system for effective long-lasting tumor treatment. It has been shown that innate immune cells, such as dendritic cells (DCs), can detect early cancerous cells upon presentation of tumor-associated neoantigens or through sensing tumor-derived pathogen or tissue injuries-associated molecular patterns according to the recognition of pathogen-associated molecular patterns (PAMP) or damage-associated molecular patterns (DAMP), respectively, by the crosstalk with pattern recognition receptors (PRRs), leading to activation of the adaptive immune responses (Fuertes *et al.*, 2011; Schreiber, Old and Smyth, 2011; Spranger *et al.*, 2017). These interactions induce proinflammatory responses by the release of cytokines such as TNF, chemokines and type I interferons associated with DC maturation and trafficking to lymph nodes, where antigen-specific T cells will be primed and activated. Consequently, T cells move and infiltrate the tumor bed through chemokine and cytokine and mediate tumor eradication. The killed cancer cells, in turn, will release additional tumor-associated antigens to increase the capacity of the response in subsequent round of the previous cycle (Chen and Mellman, 2013). To prevent the autoimmunity consequences resulted from this immunity cycle, there are balance between the activation of effector T cells and regulatory T cells to control the immune response and to distinguish between the self and non-self or between the cancer and normal cells.

Unfortunately, the aforementioned scenario may not be applied always. Types of tumors, according to their site or complexity, might be elusive to be infiltrated by effector T cells, or cancerous cells can even inhibit the immune responses through the immune checkpoints such as PD1 or CTLA4 pathways. Moreover, antigens presented or released by cancer cells can be treated as self-molecules leading to triggering of T regulatory cell responses (Motz and Coukos, 2013; Buchbinder and Desai, 2016).

Cancer immunotherapy is a rapidly developing field with a high potential to provide a cure for difficult to treat cancers. Agoists of TNFRs are one of the most promising novel groups of

immunotherapeutic reagents under consideration (Bodmer *et al.*, 2002). TNFRs and their ligands are, amongst other molecules, naturally involved in the regulation of innate and adaptive immune responses (Bodmer *et al.*, 2002). Additional approaches of immunotherapy include adoptive T cell therapy and antibody therapy. However, the efficacy of these treatments still faces obstacles to treat solid cancers.

### 1.4.1. Anti-TNFR antibodies

It has been reported that many TNFRs, including the immunotherapeutic interesting immune stimulatory receptors such as 4-1BB, CD27, OX40, TNFR2 and fibroblast growth factor inducible 14 (Fn14), are only robustly stimulated by their membrane-bound ligands but less or not by the soluble variants (Wajant, 2015). Thus, there are obstacles in the development of agonistic recombinant soluble TNFSF ligands, in addition to limited agonism, stability, and pharmacokinetics (Beutler, Milsark and Cerami, 1985; Kelley *et al.*, 2001; Medler *et al.*, 2019).

Agonistic antibodies targeting TNFRs are therefore considered as useful alternative reagents to activate TNFRs. Unfortunately, IgG antibodies targeting the aforementioned subgroup of TNFRs, which do not or only poorly respond to soluble ligand trimers, in most cases lack agonistic activity. Instead, FcγR binding, a plasma membrane-associated mode of action, is required for these antibodies in order to act as agonists and to stimulate effectively receptor signaling (Wajant, 2015). However, the FcγR binding´s dependency of the antibodies targeting TNFRs restricts their desirable immune stimulatory efficacy by prompting antibody-dependent cellular cytotoxicity (ADCC), complement-dependent cytotoxicity (CDC) or anti-inflammatory FcγRIIb activities. It has been shown that “activating” cell surface anchoring of IgG antibodies using FcγRs can be replaced by fusing antibodies with anchoring domains that recognize cell surface exposed structures distinct from FcγRs (Medler *et al.*, 2019). For example, anti-Fn14 antibody fusion proteins with a CD19- or CD20-specific anchoring domain showed strong Fn14 agonism when bound to their anchoring target (Medler *et al.*, 2019) (**Figure 6**).

The complexity of some type of tumors such as the solid types, where the spontaneously active immune reaction is elusive, necessitated the need to develop new agonistic antibodies to harness the innate and adaptive anti-tumor immunity.

Agonistic CD40 antibodies have been shown to substitute the T cell effect provided by CD4+ lymphocytes in murine models of T cell-mediated immunity. Additionally, stimulation of CD40 on tumor cells results in apoptosis in vitro and impaired tumor growth in vivo. Moreover, treatment with CD40 agonism antibody showed promising response rates and increased T cell infiltration and activation in patients with melanoma (Bajor *et al.*, 2018). CD40 monoclonal antibodies (mAbs) can even trigger direct tumor cell death via antibody-

dependent cellular cytotoxicity (ADCC) in malignancies exposed CD40, such as chronic lymphocytic leukemia (Luqman *et al.*, 2008; Khubchandani, Czuczman and Hernandez-Ilizaliturri, 2009). In the ongoing clinical trial of CD40 antibodies, there was minimal response, encouraging the design of combination therapy studies (Moran, Kovacsovics-Bankowski and Weinberg, 2013).

4-1BB agonist antibodies treatment can play a role on 4-1BB+ endothelial cells to increase T cell recruitment into tumor sites and sites of inflammation (Palazón *et al.*, 2011). To overcome the liver toxicity caused by the treatment using anti 4-1BB antibodies, combination of 4-1BB agonists with other therapeutic agonists could potentiate stronger anti-tumor responses while necessitating reduced dosing, which leads to limiting severity of 4-1BB associated adverse events. The unique and often synergistic advantages of 4-1BB activation in combination with other therapies, however, suggest an effective role in the treatment of multiple types of cancer (Bartkowiak and Curran, 2015).
Moreover, the off tumor activation of CD40 and 41BB may cause dose limiting systemic inflammation.

### 1.4.2. Inhibition of types of TNFRs and other Pro-inflammatory Cytokines to overcome groups of Autoimmune Diseases

Human disease caused by chronic inflammation, termed as autoimmune diseases, can lead to loss of function of a joint, a blood vessel or an entire organ. This chronic inflammation, caused by unsuppressed acute inflammation, can be lethal.

TNFα is involved in diversity of immunological pathways and interactions. It is thus implicated in control of the inflammation, anti-tumor responses, and immune system homeostasis. However, TNF has also been involved in tumorigenesis, diabetes, transplant rejection, septic shock, bone resorption and rheumatoid arthritis (Aggarwal, 2003; Croft, 2009; Mehta, Gracias and Croft, 2018). Furthermore, it has been demonstrated that autoimmune diseases can be associated with high levels of TNFα and soluble TNFRs in circulation (Faustman and Davis, 2013). These facts suggested that TNFα might play a critical role in the development of many chronic inflammatory diseases (Jang *et al.*, 2021). Indeed, blocking of TNF can be an effective treatment of TNF-linked autoimmune diseases (Parameswaran and Patial, 2010). However, systemic blocking of TNF-alpha can cause side effects such as among other increased risk of infection, blood disorders and heart failure.

Interleukin-1 (IL-1) is also involved in innate immunity but can also damage tissues.

The activity of interleukin-1 family members is associated with damaging inflammation. However, this cytokine family also plays a critical role in innate immunity against infections and foreign antigens. Recent therapeutic monoclonal antibodies blocking IL-1 activity are

considered as an effective treatment to reduce the severity of many autoinflammatory diseases such as type 2 diabetes (Larsen *et al.*, 2007), heart failure (Abbate *et al.*, 2010) and loss of hearing (Goldbach-Mansky, 2011). IL-1β is the most important member of the interleukin-1 family (Dinarello, 2011). It has been shown that leukocytes in patients with autoinflammatory diseases release higher level of IL-1β than cells in healthy individuals (Gattorno *et al.*, 2007). Furthermore, the abnormality in the amount of IL-1β can be associated with mutations in the intracellular proteins that control caspase 1, the enzyme that maturates the precursor of IL-1β into an active cytokine before its release from the cell (Aksentijevich *et al.*, 2002).

Canakinumab is one of the most effective therapies of autoinflammatory diseases, it is a human IgG1 monoclonal antibody targeting specifically IL-1β, and it has thus no crosstalk binding with other characterized IL-1 family members, including IL-1α and IL-1Ra (Paul M Ridker *et al.*, 2017; De Benedetti *et al.*, 2018). Canakinumab like other immune inhibitory therapeutics might associate with common adverse events, especially that it has long half-life of 30 days which allowed dosing every 8 weeks. The systemic side effects caused by canakinumab, which were independent of the delivery method either subcutaneously or intravenously, include serious infections like measles, pneumonia, varicella, urosepsis, and gastroenteritis. This highlights the need for careful monitoring of patients administrated to this therapy (Paul M. Ridker *et al.*, 2017).

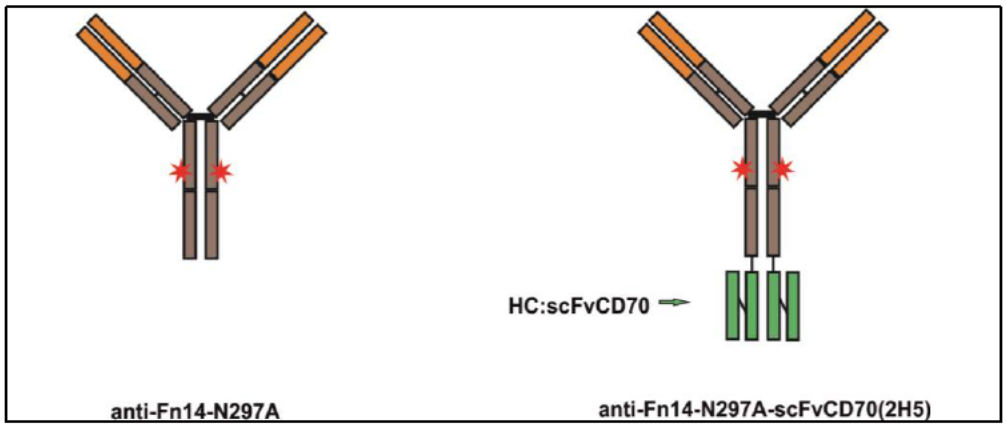


**Figure 6: Schematic representation of anti-Fn14 IgG conventional antibody fused or not with scFvCD70**

The fusion protein was fused at the C terminal domain with single chain variable domain targeting CD70 as anchoring domain, the point mutation N297A was induced to prevent the binding with Fc receptors.

### 1.5. Aim of the work

The aim of this work was the evaluation of the benefits of grafting gold nanoparticles with variants of antibodies targeting different TNF receptors. To get a stable system, the conjugation should be based on covalent bonds between the particles and the protein molecules. In particular it should be verified whether this immobilization results in agonistic activity in comparison to "free" inactive antibodies by mimicking the effect of cell-anchored antibodies or membrane bound TNF ligands. A further aim of the work was to try to supplement cell-containing hydrogel variants with antibodies-attached AuNPs to test the bioconstruct-associated local inhibitory function of AuNPs with neutralizing antibodies.

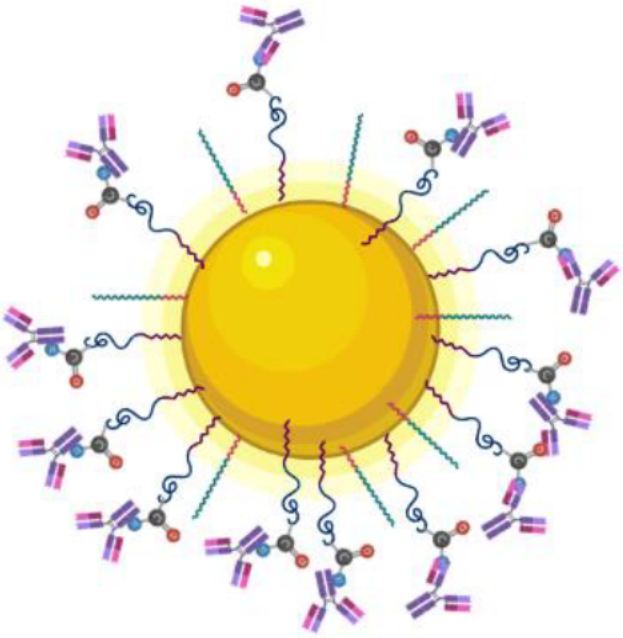


**Figure 7: Graphic illustration of the antibody-coupled gold nanoparticle.**

# 2. Material

## 2.1. Chemicals, reagents, and cell culture mediums for the cell culture

**Table 2: Chemicals, reagents and cell culture media**

| Substance | Company |
|---|---|
| Acetic acid | J. T. Baker, Leibzig, Germany |
| Acrylamide (30 %) | Carl Roth, Karlsruhe, Germany |
| Agarose | Carl Roth, Karlsruhe, Germany |
| Ammonium persulfate (APS) | AppliChem, Darmstadt, Germany |
| Ampicillin | Carl Roth, Karlsruhe, Germany |
| Anti-Flag M2 agarose beads | Sigma, Deisenhofen, Germany |
| Bovine serum albumin (BSA) | Sigma, Deisenhofen, Germany |
| Crystal violet (CV) powder | Carl Roth, Karlsruhe, Germany |
| Cycloheximide (CHX) | Sigma, Deisenhofen, Germany |
| Dimethyl sulfoxide (DMSO) | Carl Roth, Karlsruhe, Germany |
| DMEM medium | PAA, Pasching, Austria |
| Ethanol | J. T. Baker, Leibzig, Germany |
| Ethidium bromide | Carl Roth, Karlsruhe, Germany |
| Ethylenediaminetetraacetic acid (EDTA) | Carl Roth, Karlsruhe, Germany |
| 1-ethyl-3-(3-dimethylaminopropyl) carbodiimide hydrochloride (EDC) | Thermo Scientific™, Erlangen, Germany |
| Fetal bovine serum (FCS) | PAA, Pasching, Austria |
| Flag peptide | Sigma, Deisenhofen, Germany |
| Gold (III) chloride acid trihydrate | VWR International, Sťříbrná Skalice, Czech Republic |
| Killer-TRAIL | Sigma, Deisenhofen, Germany |
| mPEG-SH/mPEG-Thiol (5 kDa) | Biochempeg, Watertown, MA, USA |
| Methanol | PAA, Pasching, Austria |

**Table 2 continued: Chemicals, reagents, and cell culture media**

| | |
|---|---|
| 2-(N-morpholino) ethane sulfonic acid (MES), anhydrous ≥99% | VWR chemicals, Darmstadt, Germany |
| N-hydroxysuccinimide(1-hydroxy-2,5 pyrrolidinedione) (NHS) | Sigma-Aldrich, Schnelldorf, Germany |
| Nonfat dried milk powder | J. T. Baker, Leibzig, Germany |
| Paraformaldehyde | Sigma, Deisenhofen, Germany |
| Penicillin-Streptomycin (100 x) | Carl Roth, Karlsruhe, Germany |
| Phosphatase inhibitor II | Carl Roth, Karlsruhe, Germany |
| *Phosphate buffered saline* (PBS) | Sigma-Aldrich, Darmstadt, Germany |
| Pre-stained protein marker (broad range) | InvivoGen, Toulouse, France |
| Protease inhibitor cocktail | Biomol, Hamburg, Germany |
| Blue Protein standards | New England Biolabs, Frankfurt, Germany |
| RPMI 1640 Medium | Roche, Mannheim, Germany |
| Silver gel marker (low molecular weight) | PAA, Pasching, Austria |
| *Sodium dodecyl sulfate (SDS)* | GE Healthcare, Garching, Dassel, Germany |
| *Sucrose* | Carl Roth, Karlsruhe Garching, Germany |
| *Tetramethyl ethylenediamine* (TEMED) | Sigma, Deisenhofen, Germany |
| *SH-PEG-COOH/Thiol-PEG-Acetic Acid (5 kDa)* | Biochempeg, Watertown, MA, USA |
| *Trisodium citrate* | Thermo Scientific™, Erlangen, Germany |
| Tris | Sigma, Deisenhofen, Germany |
| *Trypsin-EDTA solution (10X)* | Sigma, Deisenhofen, Germany |
| Tween-20 | PAA, Pasching, Austria |
| β-Mercaptoethanol | Carl Roth, Karlsruhe, Germany |
| GelMA A | CELLINK, California, USA |
| Crosslinking Agent | CELLINK, California, USA |

## 2.2. Antibodies

**Table 3: Antibodies**

| Antibody | Source | Company |
|---|---|---|
| Anti-Flag mAb M2 | Mouse IgG1 monoclonal | Sigma, Deisenhofen, Germany |
| Anti-mouse IRDye 800 | Goat polyclonal | LI-COR Bioscience, Bad Homburg, Germany |
| Anti-mouse-HRP | Rabbit polyclonal | Dako-Cytomation, Denmark |
| Anti-rabbit-HRP | Goat polyclonal | Dako-Cytomation, Glostrup, Denmark |
| Anti-rabbit-HRP | Goat polyclonal | Cell Signaling Technology, Beverly, MA, USA |
| Humira (anti-TNF alpha adalimumab) | Human monoclonal | Gift from Prof. H.-P. Tony (University Hospital Würzburg) |
| Anti-TRAF1 | Rabbit monoclonal | Cell Signaling Technology, Beverly, MA, USA |
| Anti-TRAF2 | Rabbit monoclonal | Cell Signaling Technology, Beverly, MA, USA |
| β-actin | Mouse monoclonal | Sigma-Aldrich, Darmstadt, Germany |
| Cosentyx® (anti-IL-17A secukinumab) | Human monoclonal | Gift from Prof. H.-P. Tony (University Hospital Würzburg) |

## 2.3. Kits

**Table 4: Kits**

| Kit | Company |
|---|---|
| OptEIA™ IL8-ELISA | BD Biosciences, Heidelberg, Germany |
| Pierce ECL Western Blotting Substrate | Fermentas, St. Leon-Rot, Germany |
| Pierce® Silver Stain | Fermentas, St. Leon-Rot, Germany |
| Pure Yield Plasmid Midi prep System | Promega, Mannheim, Germany |

## 2.4. Instruments and disposable materials/equipment

**Table 5: Instruments and disposable materials/equipment**

| Instrument or material/equipment | Company |
|---|---|
| 96-well ELISA plates (high binding) | Greiner, Frickenhausen, Germany |
| Agfa Curix 60 processing maschine | Agfa, Düsseldorf, Germany |
| Casting chambers for SDS-PAGE | PeqLab, Erlangen, Germany |
| Cell culture bottles | Greiner, Frickenhausen, Germany |
| Cell culture petri dishes | Greiner, Frickenhausen, Germany |
| Cell culture plates | Greiner, Frickenhausen, Germany |
| Dialysing tubes, Viking, MWCO 15kDa | Carl Roth, Karlsruhe, Germany |
| Centrifuge Rotana 460R | Hettich, Tuttlingen, Germany |
| $CO_2$ incubator Heraeus Cell Safe | Heraeus, Hanau, Germany |
| Cryotubes | Greiner, Frickenhausen, Germany |
| Electrophoresis system | BioRad, München, Germany |
| ELISA-reader | Anthos Labtec, Krefeld, Germany |
| Eppendorf tubes, 1,5 ml und 2 ml | Eppendorf, Hamburg, Germany |
| Equibio EasyjecT Plus electroporator | PeqLab, Erlangen, Germany |
| Heat block | PeqLab, Erlangen, Germany |
| LI-COR Odyssey® Infrared Imager | LI-COR Biosciences, Lincoln, USA |
| Microcentrifuge 5417C | Eppendorf, Hamburg, Germany |
| Nitrocellulose membranes, 0,2 µM pore size | Whatman, Dassel, Germany |
| PCR-Thermocycle Primus | MWG Biotech, Ebersberg, Germany |
| Pipetus | Hirschmann Laborgeräte, Eberstadt, Germany |
| Polyallomer tubes | Seton, Los Gatos, CA, USA |
| Polypropylene tubes | Greiner, Frickenhausen, Germany |
| Power supply EPS 301 | GE Healthcare, Garching, Germany |
| Sterile filters (0,2µm) | Sarstedt, Nümbrecht, Germany |
| Sterile plastic Pasteur pipettes | Hartenstein, Würzburg / Versbach, Germany |
| Ultracentrifuge OPTIMA-L70 | Beckman Coulter, Krefeld, Germany |
| Well plates for cell culture | Greiner, Frickenhausen, Germany |
| Wet/tank blotting system | PeqLab, Erlangen, Germany |
| Whatman papers | Hartenstein, Würzburg / Versbach, Germany |

## 2.5. Preparations and buffers

**Table 6: Preparations and buffers**

| Preparation | Prescription |
|---|---|
| Assay diluent | 1 x PBS |
| | 10 % (v/v) FCS |
| Blot buffer 10x | 0,025 M Tris |
| | 0,192 M glycin |
| | 20 % (v/v) methanol |
| | pH 8,3 |
| CV staining solution | 20 % (v/v) methanol |
| | 0,5 % (w/v) CV powder |
| ELISA coating buffer | 8,4 g/l $NaHCO_3$ |
| | 3,56 g/l $Na_2CO_3$ |
| | pH 9,5 |
| Laemmli buffer (SDS-PAGE, 4 x) | 8 % (w/v) SDS |
| | 10 % β-Mercaptoethanol |
| | 40 % gycerol |
| | 0,2 M Tris pH 8 |
| | 0,04 % bromphenol blue |
| LB medium | 10 g peptone |
| | 5 g yeast extract |
| | 10 g/l NaCl |
| Lysis buffer for immunoprecipitation (IP) | I M Tris-Hcl pH 7.4 |
| | 2M NaCl |
| | 100 % glycerol |
| | 100 % triton |
| | volume adjusted to 1 L with distilled water |
| PBS | 0,02 M Na phosphate |
| | 0,7 % (w/v) NaCl |
| | pH 7,2 |
| PBST | 1 x PBS |
| | 0,05 % (v/v) tween-20 |
| PBST in milk | 1 x PBS |
| | 0,05 % (v/v) tween-20 |
| | 5 % (w/v) nonfat dried milk powder |

**Table 6 continued: Preparations and buffers**

| | |
|---|---|
| Running buffer 10x (SDS-PAGE) | 0,05 M Tris |
| | 0,38 M glycin |
| | 0,004 M SDS |
| | pH 8,3 |
| Separating gel buffer (SDS-PAGE) | 1,5 M Tris |
| | 0,015 M SDS |
| | pH 8,8 |
| Stacking gel buffer (SDS-PAGE) | 0,5 M Tris |
| | 0,015 M SDS |
| | pH 6,8 |
| TAE buffer | 2 M Tris |
| | 1 M acetic acid |
| | 0,1 M EDTA; pH 8,3 |
| TBS | 0,02 M Tris |
| | 8 % (w/v) NaCl |
| | pH 7,6 |
| TBST | 1 x TBS |
| | 0,05 % (v/v) tween-20 |
| TBST in milk | 1 x TBS |
| | 0,05 % (v/v) Tween-20 |
| | 5 % (w/v) nonfat dried milk powder |

## 2.6. Cells

### 2.6.1. Eukaryotic cells

The human cancer cell lines used for this work were already accessible in the Division of Molecular Internal Medicine, University Hospital of Würzburg.

**Table 7: Eukaryotic cells**

| Cell line | Source | Origin of cancer |
|---|---|---|
| HEK293 | *Institution's own stock* | Human embryonic kidney |
| HeLa-RIK3-FADD$_{KO}$ | Stably transfected cell line has been generated in the group of Prof. Wajant | Human cervical carcinoma |
| HT-1080 | *Institution's own stock* | Fibrosarcoma cell line |
| HT-1080-CD40 | Stably transfected cell line has been generated in the group of Prof. Wajant | Fibrosarcoma cell line |
| HT-1080-41BB | Stably transfected cell line has been generated in the group of Prof. Wajant | Fibrosarcoma cell line |
| HT-1080-TNFR2 | Stably transfected cell line has been generated in the group of Prof. Wajant | Fibrosarcoma cell line |

### 2.6.2. Prokaryotic cells

NEB 5-alpha Competent E. coli was obtained from New England Biolabs Company, Frankfurt, Germany

# 3. Methods

## 3.1. AuNPs synthesis

The protocol for AuNP synthesis was adapted from (FRENS, 1973; Kimling *et al.*, 2006) with slight modifications. In brief, 100 mL of 0.4 mM chloroauric acid solution was boiled in a clean 300 mL glass flask with stir bar. To keep the solution's volume constant, a reflux column or an aluminum foil was attached on top of the flask. The apparatus was boiled under stirring on a hot plate. Three milliliter of a 38.8 mM trisodium citrate solution was added to the chloroauric acid solution resulting in the production of spherical monodisperse gold nanoparticles with a diameter of approximately 60 nm. Au nanoparticles of other sizes were produced by changing the amount of added trisodium citrate and/or the concentration of auric salt within a range between 15 and 100 nm. Upon addition of the trisodium citrate, the color of the solution changed to blue in about 30 s and then to red in another 150 s. The color change during synthesis is attributed to the increase in the size of the gold nanoparticles as the citrate ions reduce the gold ions (Haiss *et al.*, 2007). The boiling was continued for another 10 min and then cooled to room temperature.

## 3.2. AuNPs functionalization

To modify the surface of the produced gold nanoparticles with carboxyl groups, a few milliliters of HS-PEG-COOH solution was added to the produced colloidal AuNPs to reach a concentration of 100 µg/mL of HS-PEG-COOH, and then it was mixed for one hour to ensure maximum adsorption on the nanoparticle surface. Carboxyl-modified AuNPs were centrifuged (10,000 RPM for 10 min), and then the pellet was collected in an Eppendorf tube and washed twice with mPEG (0.33 mg/mL) to remove the unreacted trisodium citrate and to ensure a complete functionalization of the un-PEGylated sites on the surface of HOOC-PEG-AuNPs and to stabilize the colloidal phase.

## 3.3. Coupling AuNPs with antibodies

The HOOC-PEG-AuNPs were then conjugated with the protein of interest according to the EDC-NHS covalent binding procedure adapted from (Staros, Wright and Swingle, 1986; Grabarek and Gergely, 1990). Briefly, purified AuNPs were resuspended in activation/coupling buffer (50 mM MES, pH 6.0) and washed with it three times. Then, 24 µL of EDC (200 mM) and 240 µL of NHS (200 mM) were added to 1 mL of the previous solution of AuNPs and incubated with stirring for 30 min at room temperature (RT). After washing particles three times with the activation/coupling buffer to remove the EDC and NHS reagents, 500 µL of the activated AuNPs were incubated with 500 µL of the antibody of interest for two hours at a temperature of 4 °C. The antibody-conjugated AuNPs were washed three times with blocking buffer (RPMI 1640 medium (0.5 % FCS- 1 % Penicillin &

Streptomycin) to remove the excess of the unconjugated protein and to block the free activated carboxyl sites on the surface of gold nanoparticles. Finally, the antibody-conjugated AuNPs were resuspended in a storing buffer (RPMI 1640 medium (1 % Penicillin & Streptomycin) for later use. For dot blot analyses, a concentration titration series of AuNPs and antibodies were dotted (1 µL) to nitrocellulose. After drying, remaining free binding sites on nitrocellulose were blocked and antibodies were detected via sequential incubation with primary antibody (anti-human IgG primary antibody (H+L) source: Mouse, Catalog # 31135), (HRP)-conjugated secondary antibodies (Anti-Mouse Immunoglobulins/HRP, #P0260, Source: Rabbit, Dako) and the commercially available ECL western blotting detection reagents and analysis system (Amersham Biosciences, Muenchen, Germany).

### 3.4. AuNP characterization

UV-vis: AuNPs samples were collected immediately after synthesis and their optical properties were evaluated via UV–vis spectrophotometry (SpectraMax). The absorption spectra were acquired in the range of 450–650 nm with a step of 5/10 nm. DLS: The size of the obtained AuNPs (unPEGylated, PEGylated, and grafted with antibodies particles) were analyzed using a Nanophox 123 by dynamic light scattering (DLS) with photon cross-correlation spectroscopy from Sympatec. The particles were purified via centrifugation at 22,000 g for 10 min, diluted 100 times in distilled water, and then analyzed. All DLS experiments were carried out at a temperature of 25 °C.

Zetasizer: The effective surface charges on the gold nanoparticles were measured as zeta-potential using a zetasizer from Malvern Instruments Zetasizer, Malvern, UK. For all measurements, AuNPs were diluted 10–100 times (depending on their concentration) in water.

### 3.5. Binding of Gaussia princeps Luciferase (GpL)-fusion proteins to antibodies immobilized on AuNPs

To determine the minimum antibody concentration needed for conjugation, increasing concentrations of easily available anti-TNF or anti-IL17A antibodies were used. The conjugated AuNPs were incubated with a constant amount of GpL-TNC-TNF for 90 min at 37 °C, and after removal of the unbound GpL fusion protein molecules by washing with PBS, AuNPs-associated luciferase activity was measured (see below). For this, particles were transferred to a black 96-well plate and 25 µL of GpL assay solution (1.5 µM Coelenterazin (Carl Roth, Karlsruhe, Germany, 4094.3) in PBS) was added. Luciferase activity was immediately measured (1 s per well) using a PHOMO Photometer (Anthos Mikrosysteme, Schwerin, Germany). Binding values calculated for anti-TNF-AuNPs served as total binding values, while binding values calculated for the anti-IL17A-AuNPs were considered as non-specific binding of GpL-TNC-TNF. To confirm the coupling of different types of antibodies to

gold nanoparticles (AuNPs), the binding of GpL-TNC-TNF or GpL fusion protein of the extracellular domain of Fn14 (Fn14ed-GpL) to the AuNP-immobilized antibodies was determined via equilibrium binding studies. For this, a serial dilution of GpL-TNC-TNF or Fn14ed-GpL was mixed with a constant amount of the antibody-conjugated AuNPs (1 mg/mL in linking solution) for 90 min at 37 °C, and after removal of the unbound GpL fusion protein molecules, AuNP particle-associated luciferase activity was measured. Binding values derived from PDL192-AuNPs or 5B6-AuNPs served as total binding values, while binding values derived from the anti-TNF-AuNPs were considered as non-specific in the case of incubation with Fn14ed-GpL. Three washing steps were performed to remove unbound proteins. The raw data obtained from the binding studies were analyzed with GraphPad Prism5 software. Total binding values and corresponding non-specific binding values were subtracted to obtain specific binding values. KD values were then calculated with the "nonlinear regression to a one-site specific binding curve" function of GraphPad Prism5.

### 3.6. Determination of IL-8 production

HT-1080 cells ($15 \times 10^3$ / well) were seeded in 96-well tissue culture plates and cultured overnight. The following day, medium was changed and cells were incubated for 16–18 h with the indicated concentrations of AuNP-immobilized anti-Fn14 antibodies, AuNPs, and trimeric soluble Flag-TWEAK with and without anti-Flag oligomerization. In the coculture experiments Fc receptor and membrane-bound TWEAK expressing transfectants or HEK293 cells transfected with empty vector as a control were added at a ratio of 1:1 to target cells, and 30 min later, the mixture of cells, containing Fc receptor transfectants or HEK293 cells transfected with empty vector, was challenged with anti-Fn14 antibody. Similar steps were performed in the case of other types of AuNPs-immobilized antibodies, in which cells expressing the related receptors were challenged with relevant AuNPs-Ab, irrelevant AuNPs-Ab (control particles), soluble antibody of interest, and the related Flag-tagged ligand with or without anti-Flag oligomerization. Likewise, HT-1080 cells, which lack of the studied receptor, were stimulated to confirm the specificity of the antibodies. At 16–18 h post stimulation, supernatants were collected and analyzed with respect to their IL-8 content using the non-competing anti-IL-8 sandwich antibody pair of the BD OptEIA™ human IL8-ELISA kit (BD Biosciences, NJ, USA) according to the manufacturer's instructions.

### 3.7. p100 to p52 Processing and western blotting Analysis

HT-1080 cells ($1 \times 10^6$ / well) were seeded in 6-well plate and cultivated overnight. Cells were then treated with AuNPs, anti-Fn14 antibodies, and AuNPs-immobilized anti-Fn14 antibodies. As a positive control, cells were also stimulated with Flag-TWEAK (Roos *et al.*, 2010). The next day, cells were collected using a rubber policeman and the remaining medium was removed via two washes with ice-cold phosphate buffered saline (PBS). Total

cell lysates were then prepared in 4× Laemmli sample buffer (8% SDS, 0.1 M DTT, 40% glycerol, 0.2 M Tris (pH 6.8), 0.004% bromophenol blue) supplemented with complete protease inhibitor (Roche Applied Science, Grenzach-Wyhle, Germany) and phosphatase inhibitor mixtures I and II (Sigma-Aldrich, Schnelldorf, Germany) via sonication (10 pulses for 20 s) and boiling (95 °C, 5 min). Lysates were cleared via centrifugation (14,000 rpm, 4 °C, 10 min) and separated using sodium dodecyl sulfate (SDS) polyacrylamide gel electrophoresis on 12.5% gels. After transfer to nitrocellulose TRAF1 induction, TRAF2 degradation and p100 to p52 processing were analyzed using western blotting. In brief, free protein binding sites on the nitrocellulose were blocked for 1 h in Tris-buffered saline containing 0.1% Tween 20 and 5% dry milk and proteins of interest were detected via sequential incubation with primary antibodies: (anti-TRAF1 mAb, (45D3) #4715, Source: Rabbit; anti-TRAF2 mAb, Source: Rabbit, (C192), #4724) from Cell Signaling, MA, USA; anti-NF_B p100/p52 mAb, Source: Mouse, #05-361 from Millipore, Darmstadt, Germany; anti-ß-actin mAb, Source: Mouse, clone AC-15, #A1978 from Sigma-Aldrich, Schnelldorf, Germany, horseradish peroxidase(HRP)-conjugated secondary antibodies: (Anti-Mouse Immunoglobulins/HRP, Source: Rabbit, #P0260 from Dako, Hamburg, Germany; Anti-rabbit IgG, HRP-linked Antibody, Source: Goat, #7074, Cell Signaling, MA, USA), and the commercially available ECL western blotting detection reagents and analysis system (Amersham Biosciences, Muenchen, Germany).

### 3.8. Cell culture

For proteins production, HEK293 cells were prepared as follow, the old nutrient medium was discarded from a cell culture flask, next, 2-3 ml of trypsin-EDTA solution (1x) was added and incubated for 10 min at 37°C & 5% CO2, 7 ml of fresh RPMI 1640 medium (10% FCS) was added to inhibit the trypsin´s function. After a significant mixing of the previous mixture, 4 ml from the last total volume was seeded on a big cell culture plate for the transfection step, and 2 ml was left in the flask with 25 - 50 ml of fresh medium and incubated at 37°C & 5% CO2 for further cultivating.

For the characterization of protein functions, HT-1080, HeLa and HaCaT cells were split by washing with PBS (1x), adding trypsin-EDTA solution and incubation for 10 minutes at 37°C & 5% CO2. Then the cells were centrifuged at 1200 rpm for 4 minutes to discard the trypsinization solution and replace it with 10 ml of fresh RPMI or DMEM medium complemented with 10 % FCS. Finally, the cells were counted under the microscope using hemocytometer before seeding on 96-wells cell culture plates for further stimulation. The rest of the cells were diluted to the ratio of 1:3 till 1:10 and further cultivated in fresh medium with 10 % FCS and were regularly frozen at -80°C in 1 ml freezing medium (10 % DMSO in FCS) contained in cryotubes.

## 3.9. Production of the expression plasmid encoding antibody fusion proteins

### 3.9.1. Preparation of E. coli cultures

E. coli strains were transformed with the corresponding plasmids and cloned by help of one of my colleagues. In order to amplify the amount of required constructs, clones containing plasmids of intended proteins were cultivated in culture´s medium which prepared as follow, 30 ml of 5x medium LB was diluted with 120 ml of distilled water in Erlenmeyer flask, then,150 µl Ampicillin from a stock solution was added to each 150 ml of the culture.7µl of each E. coli strain solution was added to the related flask and incubated to grow overnight at 37°C.

### 3.9.2. Isolation of Plasmid DNA (Mini Preparation)

The previous E. coli cultures were divided to an aliquot of the bacterial suspension for long-term storage of the clone and the remaining parts of cells were harvested by centrifugation for 15 min at 6,000 × g and 4°C. The isolation of plasmid DNA was completed by using Plasmid Miniprep System from Promega following the manufacturer's instruction. The eluted DNA was finally stored at –20°C. The DNA concentration was measured photometrically at OD260 using the spectrophotometer GeneQuant *pro* from Pharmacia.

## 3.10. Protein production

The transfection reagent was prepared by mixing 36 µl of polyethylenimine (PEI) with 2 ml of serum-free RPMI medium 1% (penicillin – streptomycin) in addition to a volume of the isolated DNA construct (containing 12 µg of DNA of interest), vortex step was then carried out, and the total reagent was incubated at room temperature for 10 min, during the incubation period, the old medium of the HEK293 plates was removed and replaced by 17 ml of serum-free RPMI medium 1% (penicillin – streptomycin). Finally, the transfection reagent was added to each corresponding plate gently on the plate´s wall to avoid damaging the cultured cells, the plates were incubated overnight at 37°C & 5% CO2.

On the next day, the medium with the transfection reagent were discarded and replaced by 15 ml of RPMI containing 2% FCS and 1% (penicillin – streptomycin), the plates were incubated for 6 to 7 days at 37°C & 5% CO2. After 7 days, the supernatants were collected and centrifuged at 4600 rpm for 10 min to remove the dead cells and debris. The amount of protein production was detected by measuring the protein concentration using LI-COR Odyssey® Infrared Imaging system (see 3.13).

## 3.11. Protein purification

The supernatants produced by HEK293 cells containing Flag-tagged proteins were purified using affinity chromatography on anti-Flag M2 agarose beads. Anti-FLAG M2 antibody

agarose was poured on the column slowly to abrogate formation of any air bubbles after washing by sterilized PBS buffer 2 times followed by centrifuging step in each time, then 6 ml of glycine solution (0.1 M) 2.5 PH in TBS was poured on the bead. The bead was kept wet by excess of TBS buffer. The centrifuged collected supernatant of the produced protein was poured gently on the beads through two steps by flow rate of at least drop/40-45 sec. Finally, the whole set was stored overnight in 4° C. Afterwards, the beads were washed with TBS and the bound protein molecules were eluted from the beads in 0,7 ml fractions using 6 ml of FLAG peptide in TBS (100 µg/ml) and the flow rate was at least one drop/min. The eluted proteins were dialyzed against PBS overnight at 4 °C and then sterile filtered on the next day and stored at -20 °C for further analysis. The percent of protein recovery after purification was controlled by measuring the protein´s concentration in all the followings: the supernatant before purification, the flow-through, the elution-fractions, the TBS washing flow-through after purification and beads using SDS-PAGE & Western blot analysis followed by LI-COR Odyssey® Infrared Imaging system as described in (see section 3.13).

### 3.12. Silver staining.

The purified proteins were separated by SDS-PAGE and the gel was stained using Pierce® Silver Stain Kit according to the instruction of the manufacturer.

### 3.13. SDS-PAGE and detection the concentrations of proteins.

#### 3.13.1. SDS-PAGE

SDS-PAGE gels were prepared for separation of the proteins. First, the separating gel was prepared from 0,374 M Tris (pH 8,8), 0,0035 M SDS, dis. H2O 12 % and 10 % acrylamide, and then polymerized using 0,1 % APS and 0,1 % TEMED. Immediately after pouring the gel and before its polymerization, isopropanol was added on the surface of the separating gel to acquire a straight surface. After polymerization, isopropanol was discarded and the stacking gel was directly poured on the prior gel this stacking gel was made up of 6 % acrylamide in 0,123 M Tris (pH 6,8), 0,00375 M SDS, 0,1 % APS and 0,1 % TEMED. The sample wells were formed in the stacking gel before polymerization by using a comb. After polymerization, the comb was removed, and the samples were added using micropipette to run electrophoretic separation at 120 V and 400 mA for 95 min in case of small gels and 105 min in case of large gels.

#### 3.13.2. Blotting on nitrocellulose membrane

Once the electrophoresis has done, western blotting of the gel on a nitrocellulose membrane was performed by applying an electrical current 90 v, 400 mA for 2:30 hour using Wet/tank blotting system, the blotting process was started by pressing the nitrocellulose membranes

directly on the gel in the blotting chamber as a sandwich in the following order: anode - 2 wet Whatman papers - nitrocellulose membrane- gel - 2 wet Whatman papers -cathode.

### 3.13.3. Membrane´s visualizing and calculation of protein´s concentration

Next, the remaining binding sites on the membrane were blocked with a 5% milk solution in Tween-TBS buffer for 1 hour at room temperature and washed with Tween-PBS buffer 3x for 10 min, then, primary anti-FLAG antibody was incubated with the membrane overnight at 4 °C on a shaker.

On the next day, the membrane was washed again 3x with TBS or PBST for 30 min, afterwards it was incubated with secondary antibody in PBST or TBST-milk for 1h at room temperature on the shaker. Finally, the membrane was washed 3 times with PBST or TBST for 30 min and then developed using antibody anti-mouse IRDey 800, then the membrane was scanned by LI-COR Odyssey® infrared imaging, proteins´ concentrations were calculated through a comparison with standard purified FLAG-containing proteins of known concentration.

## 3.14. Cell viability assay

Hela-RIP3-$FADD_{KO}$ cells [26] ($20 \times 10^3$ / well) were seeded in 96-well tissue plates. The next day, cells were treated in the presence or absence of TNF (1 ng/mL) with AuNP-immobilized anti-Fn14 antibodies, AuNPs, or Flag-TWEAK. Cell viability was determined after an additional 18 h via crystal violet staining of the remaining attached viable cells to the plate after discarding the supernatant from the plates and adding 70 µl/well of the CV staining solution. The plates were left for 20 minutes at room temperature. Afterwards, the excess of CV staining was removed by washing two times with distilled water. The plates were left to dry at room temperature, (Feoktistova, Geserick and Leverkus, 2016).

Finally, the plates were measured at 595 nm. To normalize cell viability values, each plate included a triplicate of untreated cells considered as 100 % viable and a triplicate of cells challenged with a cytotoxic mixture (400 ng/ml TNF, 400 ng/ml CD95L 400 ng/ml TRAIL, 25 µg/ml CHX, 1 % (w/v) sodium azide) producing maximal cell death to deliver the value for 0 % viability. All other viability values were normalized according to the averages of these triplicates and analyzed by the Graph Pad Prism 8.2.0 software (La Jolla, CA, USA).

## 3.15. ICP-MS measurement of Au in the hydrogel

Sample of GelMA A-AuNPs with or without cells were dissolved (100 µl) in 900 µl HCl suprapur (30%) overnight and then 9 ml 0.69% HNO3 solution (suprapur) were added. The blank (which was substracted from the measurements as well as the standard solutions) was prepared my mixing 1ml HCl suprapur with 9 ml 0.69% HNO3 solution (suprapur).

The samples were measured with an iCAP RQ ICP-MS (Thermo Fisher Scientific) in He collision mode. The internal standard Rh with a concentration of 10 ppm was added to each sample. During the measurement of one sample, the ICP-MS measures three times and outputs the average.

### 3.16. Statistical analysis

All presented figures in this current work were designed by Microsoft Office Excel 365 pro plus, GraphPad Prism 8.2.0 program and CorelDRAW Graphics Suite 2018 software, in addition to the scientific image and illustration website **biorender.com**.

# 4. Results

## 4.1. Size and Concentration of Gold Nanoparticles can be Controlled by Auric Salt to Reducer Ratio

Based on the fact that the size of AuNPs can be controlled according to the concentration of the auric salt ($HAuCl_4 \cdot 3H_2O$) (FRENS, 1973). We optimized the procedure for the preparation of AuNPs to obtain AuNPs with a size below 200 nm. For this purpose, the trisodium citrate concentration was fixed to 38.8 mM but the concentration of gold chloride and boiling duration were varied. A gold chloride concentration of 0.4 g/L to 1.6 g/L and boiling duration of 10 min was used in the first experiment (**Figure 8**A). In a second experiment 0.4 g/L of gold chloride was used and the boiling duration was varied from 5 to 40 min (**Figure 8**B). UV-vis absorption was used to characterize the size of the particles. The wavelength of the maximum absorbance of the plasmon band of the spherical gold nanoparticles is related with the size of the particles (Haiss *et al.*, 2007; Amendola *et al.*, 2017). As shown in **Figure 8**A, increasing the concentration of the gold chloride led to a lambda max shift from 520 nm to 550 nm, indicating an increase of particle size from 15 nm to 80 nm. On the other hand, different results were observed for the influence of the boiling duration. As shown in **Figure 8**B, the optical density increased with fixed λmax absorbance indicating that the total amount

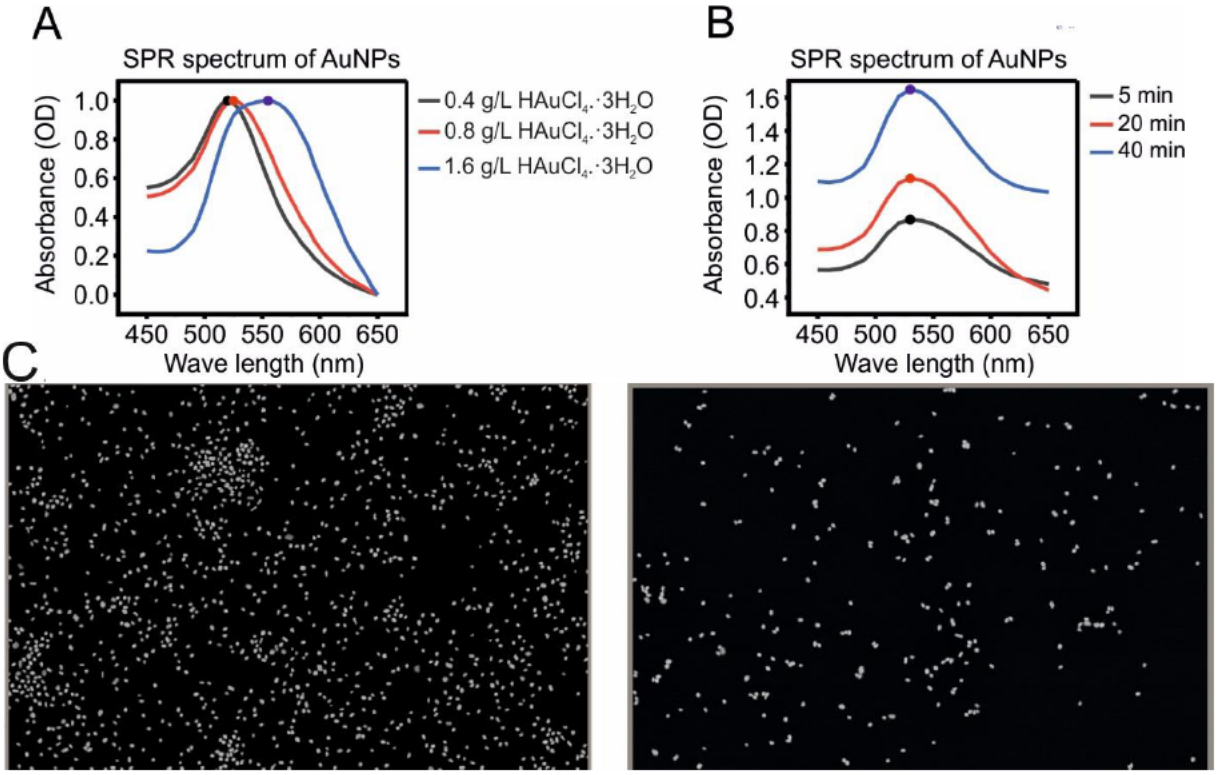


**Figure 8: UV-visible absorption spectrum and SEM visualization of gold colloids AuNPs.**

Particles were prepared with (A) different concentrations of $HAuCl_4.3H_2O$ or (B) different boiling duration with fixed concentration of $HAuCl_4.3H_2O$. (C) SEM images of AuNP suspension in MilliQ® water.

of the produced gold nanoparticles increased with extended boiling time (Haiss *et al.*, 2007). Moreover, the produced particles have spherical shape and resembled the shape of commercial particles of the same size (**Figure 8**C). In sum, these initial experiments demonstrated that the gold nanoparticle size can be controlled by changing the initial concentration of the $HAuCl_4$. For all further experiments, 0.4 g/L of $HAuCl_4$ and a boiling duration of 10 min was used to generate AuNPs by the Turkevich synthesis method.

### 4.2. Functionalization of the Gold Nanoparticles

Trisodium citrate plays a role as reducing agent and as stabilizer of the produced gold nanoparticles (Oliveira *et al.*, 2020). The abundance of negative charges of the citrate structure surrounding the surface of AuNPs is known to maintain the colloidal state and the mono dispersion. However, the stabilizing effect of citrate is not durable enough for storing the particles for long-term and can be lost after purification. To increase the long-term stability of AuNPs and to introduce chemical groups for subsequent conjugation reactions,

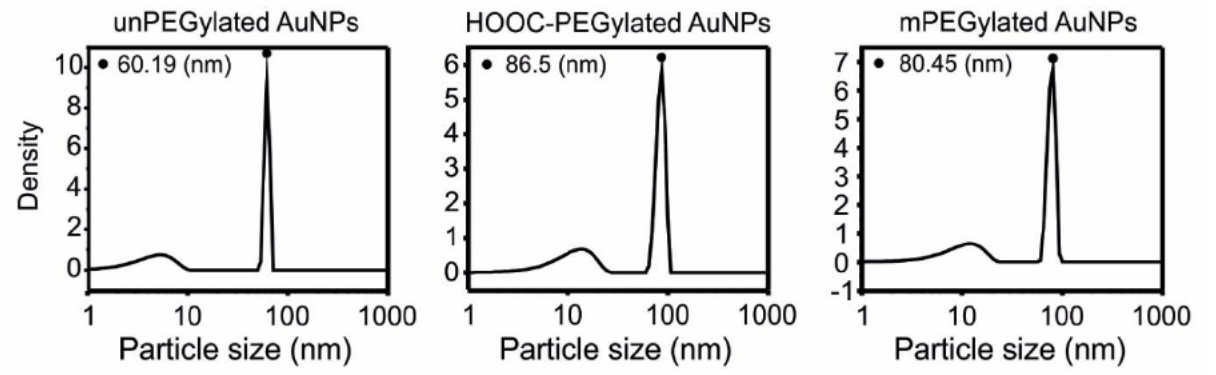


**Figure 9: Specific binding of Fn14ed-GpL fusion protein to 5B6-AuNPs and PDL192-AuNPs.**

Three equal amounts of carboxyl-modified gold nanoparticles AuNPs (25 mg/mL) were conjugated with a constant concentration (2 mg/mL) of the anti-Fn14 antibodies 5B6 (A) and PDL192 (B) or anti-TNF as a negative control. After removal of unbound antibody molecules, the antibody-AuNP conjugates were incubated with the indicated concentrations of the Fn14ed-GpL fusion protein for an hour at 37 °C. After removal of the unbound Fn14ed-GpL molecules, nonspecific binding values were obtained from the anti-TNF-AuNPs and were subtracted from the corresponding total binding values obtained from the 5B6-AuNPs and PDL192-AuNPs to calculate the specific binding values. The latter were fitted using non-linear regression to a single binding site interaction plot using GraphPad Prism5 software.

particles were functionalized with a layer of carboxyl-(5 kDa HOOC-PEG-SH) or methoxy- (5 kDa H3C-O-PEG-SH) containing polymers. Grafted particles were purified by washing with distilled water to discard the excess of trisodium citrate and free polymer molecules. The particle size after grafting with carboxyl-PEG and methoxy-PEG were then characterized using DLS (Dynamic Light Scattering). The increase of particles size after PEGylation with two types of polymers was similar, from approximately 60 to approx. 86 nm and 80 nm, respectively (**Figure 9**). This is most likely due to the identical molecular weight of the grafted polymers. The small peak in the range of ±10 nm is a false peak resulting from the effect of the rotational diffusion in the case of the large particles > 40 nm which scatter strongly

(Khlebtsov and Khlebtsov, 2011). To confirm the PEGylation, zeta potential measurements were performed. As shown in **Table *8***, the PEGylation led to a change in ζ potential values. In comparison to the citrate stabilization, the charge of the particles after PEGylation with carboxyl-PEG is even more negative (-20 mV), while after the grafting with methoxy-PEG it is less negative (-7 mV).

**Table 8: Comparation of ζ potential values and particles size between the non-PEGylated and PEGylated gold nanoparticles.**

| Sample | Particle Size | ζ Potential |
|---|---|---|
| Trisodium citrate-AuNPs | 60 ±0.2 nm | −14 mV |
| mPEG-AuNPs | 80 ±2 nm | −7 mV |
| HOOC-PEG-AuNPs | 86 ± 3 nm | −20 mV |

### 4.3. Conjugation of HOOC-PEG-AuNPs with Therapeutic Antibodies

Carboxyl-modified gold nanoparticles (HOOC-PEG-AuNPs; ca. 25 mg/mL) were initially conjugated with the commercially available antibodies adalimumab (anti-TNF) and secukinumab (anti-IL17) to establish the coupling conditions. Please note that from now on AuNPs refers to the carboxyl-modified gold nanoparticles. The conjugation process was performed using EDC/NHS coupling reaction. To confirm the post-conjugation functionality of anti-TNF, binding studies using GpL-TNC-TNF were performed. The GpL domain allows the quantification of the binding of the GpL-TNC-TNF molecules to the gold nanoparticle-associated antibodies via measurement of the particle-associated luminescence upon removal of the free GpL fusion protein molecules. The binding of GpL-TNC-TNF to anti-TNF-AuNPs was considered as total binding and the binding to anti-IL17A-AuNPs was considered

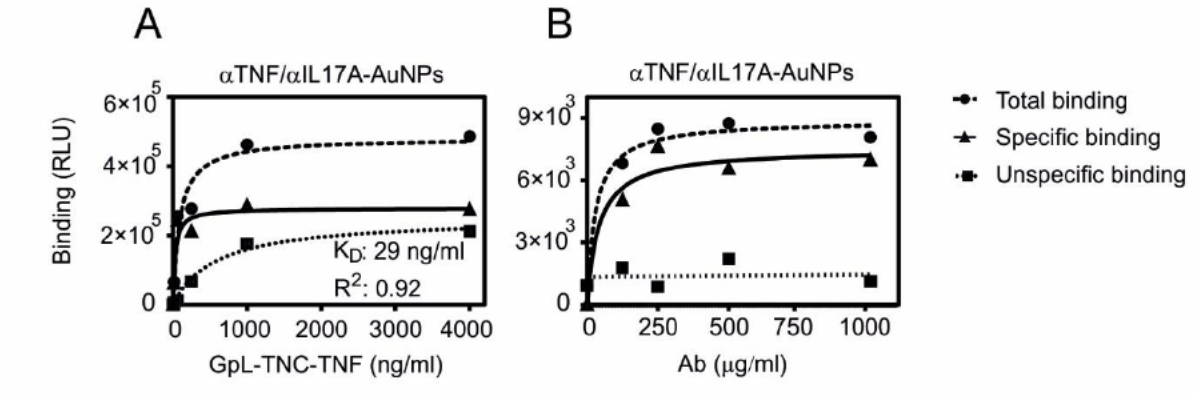


**Figure 10: Specific binding of GpL-TNC-TNF to anti-TNF-AuNPs**

Equal amounts of carboxyl modified gold nanoparticles (AuNPs; 25 mg/mL) were conjugated with a constant concentration of anti-TNF or anti-IL17A (2 mg/mL). After removal of the excess unbound antibody molecules, the antibody-conjugated AuNPs were incubated with the indicated concentrations of the GpL-TNC-TNF fusion protein for an hour at 37° C (A). Alternatively, increasing concentrations of the two antibodies were used for gold nanoparticle conjugation and were then incubated with a fixed concentration (500 ng/mL) of GpL-TNF-TNC (B). After removal of unbound GpL-TNF-TNF molecules, the nonspecific binding values (derived of the anti-IL17A-AuNPs) were subtracted from the corresponding total binding values (derived of the anti-TNF-AuNPs) to obtain specific binding values that were fitted using non-linear regression to a single binding site interaction plot using GraphPad Prism5 software.

as unspecific binding (**Figure 10**). A serial dilution of the GpL-TNC-TNF was mixed with a constant amount of the antibody-conjugated AuNPs (1 mg/mL in linking solution). As shown in **Figure 10**A, specific binding increased with higher antigen concentrations and reached a plateau with half maximal binding of ~30 ng/mL. These results suggest that the conjugation does not interfere with high affinity binding of TNF to the antibody.

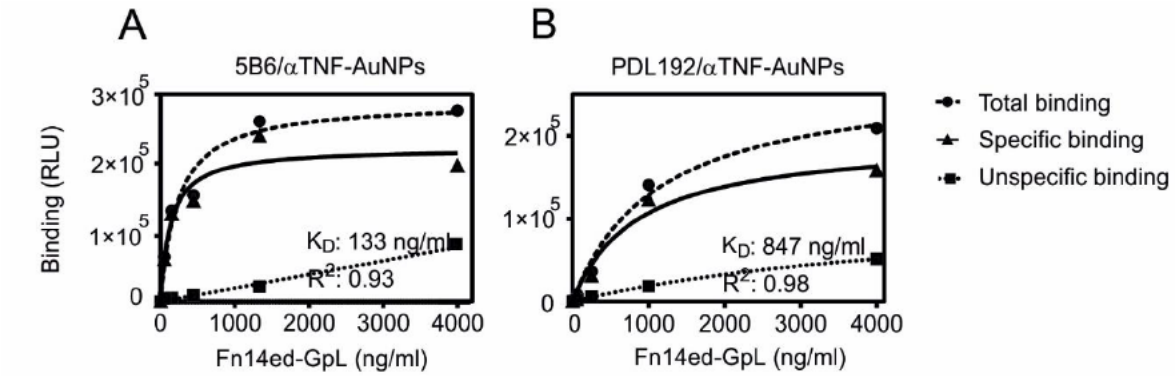


**Figure 11: Specific binding of Fn14ed-GpL fusion protein to 5B6-AuNPs and PDL192-AuNPs.**

Three equal amounts of carboxyl-modified gold nanoparticles AuNPs (25 mg/mL) were conjugated with a constant concentration (2 mg/mL) of the anti-Fn14 antibodies 5B6 (A) and PDL192 (B) or anti-TNF as a negative control. After removal of unbound antibody molecules, the antibody-AuNP conjugates were incubated with the indicated concentrations of the Fn14ed-GpL fusion protein for an hour at 37 °C. After removal of the unbound Fn14ed-GpL molecules, nonspecific binding values were obtained from the anti-TNF-AuNPs and were subtracted from the corresponding total binding values obtained from the 5B6-AuNPs and PDL192-AuNPs to calculate the specific binding values. The latter were fitted using non-linear regression to a single binding site interaction plot using GraphPad Prism5 software.

In order to evaluate to what extent, the antibody concentration used for coupling affects the amount of functional binding sites, increasing concentrations of anti-TNF or anti-IL17A were used for conjugation. The binding with a constant concentration of GpL-TNC-TNF was then determined, as shown in **Figure 10**B. With a concentration of 250 µg/mL of anti-TNF in the

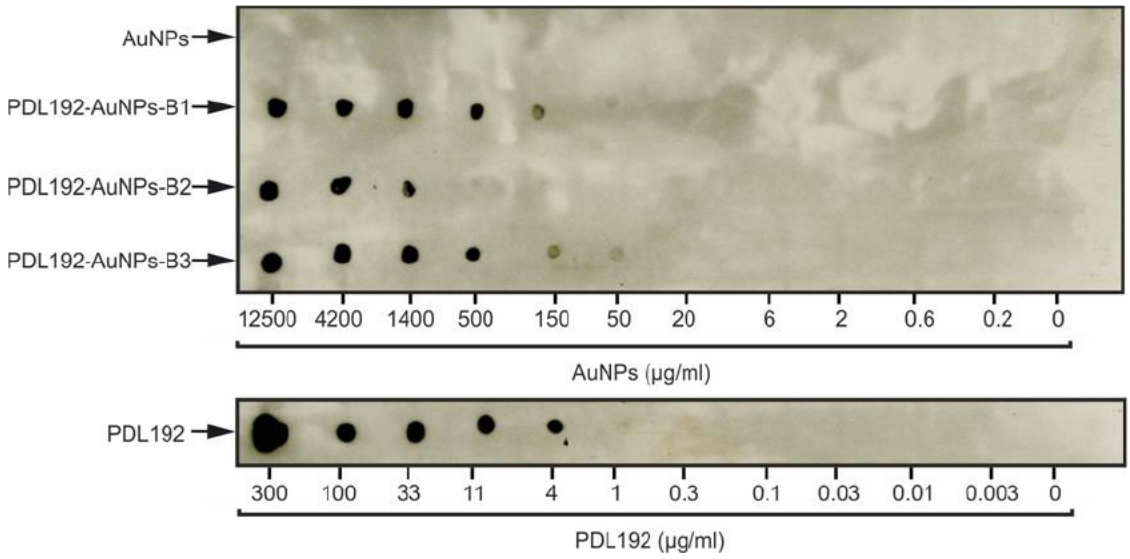


**Figure 12: Dot blot analysis.**

Concentration titration series of AuNPs, PDL192-AuNPs (three batches) and antibody only. Samples were dotted (1 µL) to nitrocellulose. Antibodies were detected by sequential incubation with primary antibody (anti-human IgG primary antibody (H+L)), (HRP)-conjugated secondary antibodies (Anti-Mouse Immuno-globulins/HRP) and the commercially available ECL Western blotting detection reagents and analysis system.

coupling reaction, the maximum amount of functional conjugated antibody was practically reached and there was no relevant improvement up to 1000 µg/mL.

Similar binding studies were then performed with AuNPs conjugated with the in-house produced anti-Fn14 antibodies PDL192 and 5B6 and Fn14ed-GpL, a GpL fusion protein of the extracellular domain of Fn14 and GpL (**Figure 11**). This time, the anti-TNF conjugated AuNPs were used to determine the unspecific binding values. Dot blot analysis confirmed the coupling of PDL192 to the gold nanoparticles in three batches and gives an estimate of the total concentration of coupled antibody independent of its functionality (**Figure 12**).

### 4.4. AuNP-immobilized Anti-Fn14 Antibodies Mimic the Mode of Action of the Membrane-bound of the Fn14 Ligand TWEAK

To characterize the effect of immobilizing of PDL192 and 5B6 on gold nanoparticles on their biological activity on Fn14 beyond binding, *in vitro* assays were performed to compare the effect of anti-Fn14-AuNPs with those of the soluble antibody variants on Fn14 signaling. Fn14 expression is frequently found to be strongly enhanced in tumor tissue and different tumor cell lines like HT1080 (Wajant, 2013; Kums *et al.*, 2017). Stimulation of Fn14 results in the activation of the classical NFκB pathway, which leads to production of the inflammatory cytokine IL-8 (Salzmann *et al.*, 2013), to enhancement of TNF-induced cell death, and to activation of the alternative NFκB pathway. It was shown that soluble TWEAK stimulates the alternative NFκB pathway and enhances TNFR1-induced cell death but only weakly triggers signaling via the classical NFκB pathway. However, membrane TWEAK, the cell bound precursor of soluble TWEAK, induces all these pathways very efficiently (Roos *et al.*, 2010). It has been furthermore demonstrated that anti-Fn14 antibodies show no agonistic activity with respect to production of IL-8 and enhancement of TNFR1-induced cell death without oligomerization with protein G or Fc receptor binding and additionally only poorly trigger p100 processing, a hallmark of alternative NFκB pathway activity (Salzmann *et al.*, 2013). We wondered whether and if yes to which extent the AuNP immobilization of the anti-Fn14 antibodies PDL192 and 5B6 can make them agonistic.

To evaluate this, we seeded HT1080 and HT1080-Fn14-knockout cells and challenged the cultures the next day for 14–18 h with dilution series of the following reagents: AuNPs, PDL192/5B6-AuNPs, and Flag-TWEAK with and without anti-Flag. Anti-Flag oligomerized Flag-TWEAK mimics hereby the action of membrane TWEAK (Wajant, 2015). In addition, we analyzed the free antibodies in the presence of FcγR-expressing cells and in comparison to membrane TWEAK-expressing cells. Finally, the supernatants were assayed for IL-8 production using ELISA. **Figure 13**A shows for three independent batches of AuNP-immobilized anti-Fn14 antibody PDL192 that the immobilized antibody triggered IL-8 production (a hallmark of the classical NFκB pathway) as efficient as anti-Flag oligomerized TWEAK. In the control group with Fn14-deficient HT1080 cells there was no increased IL-8

production confirming the Fn14 specificity of the response analyzed. Likewise, **Figure 13**B shows that the AuNP-immobilized PDL192 antibody can trigger the same maximal response as high amounts of FcγR-bound antibody and membrane-TWEAK expressing cells.

To characterize the effect of AuNP-immobilized PDL192 and 5B6 on the alternative NFκB pathway, western blot analysis of whole cell lysate of HT1080 cells stimulated with PDL192- and 5B6-AuNPs, AuNPs, and sTWEAK was performed to detect p100 to p52 processing and, in addition, induction of TRAF1 and degradation of TRAF2, which are associated with alternative NFκB signaling (**Figure 14**). We observed that AuNP-immobilized anti-Fn14 antibodies but not the soluble antibodies induce TRAF1 expression, p100 processing, and weak TRAF2 depletion in a similar fashion to sTWEAK.

Last but not least, we analyzed the ability of the anti-Fn14-AuNPs to trigger Fn14-mediated enhancement of TNF-induced necroptosis.

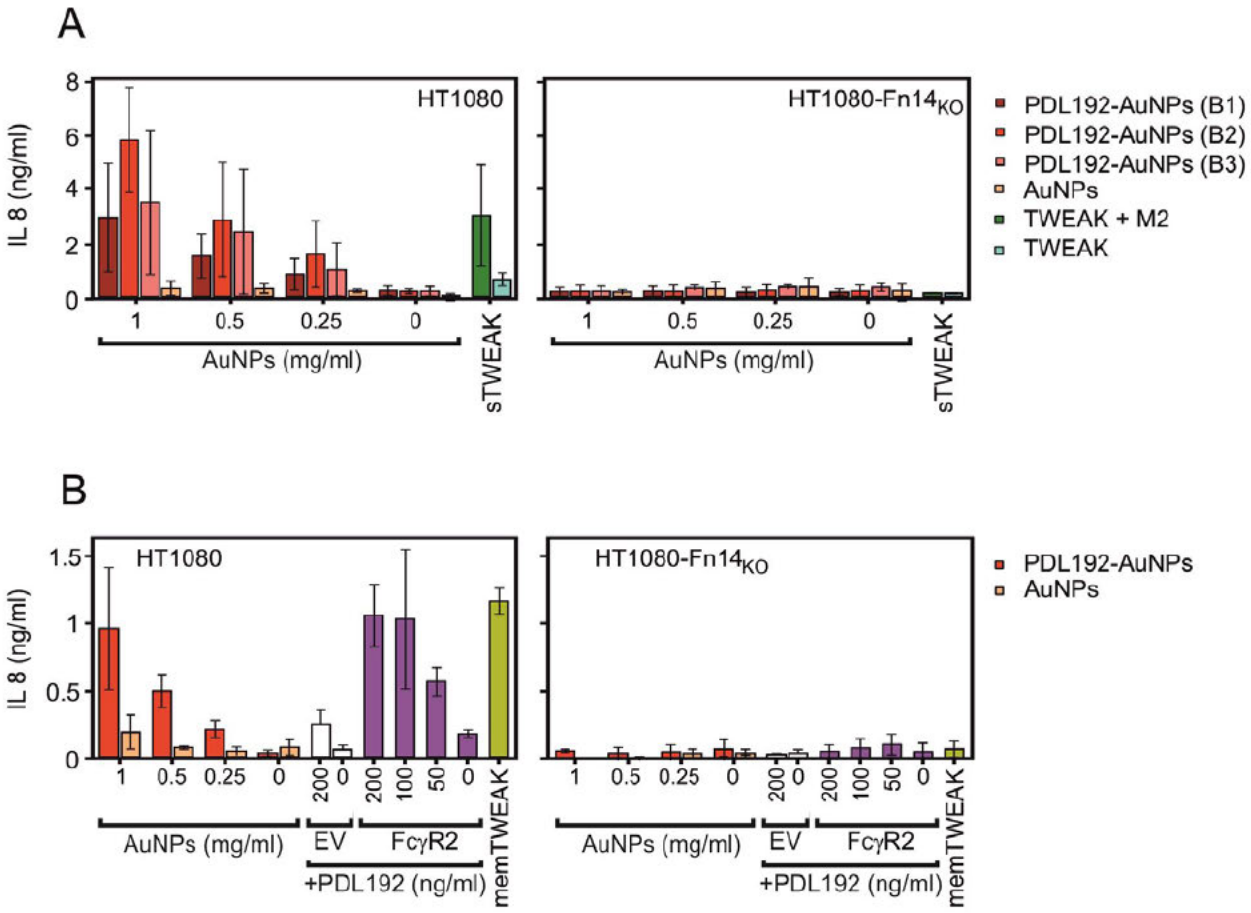


**Figure 13: AuNPs-immobilized anti-Fn14 antibody triggers IL-8 production in a similar fashion to cell-anchored antibodies or membrane-bound TWEAK.**

HT1080 or HT1080-Fn14-knockout cells ($15.10^3$/well) were seeded in 96-well plates, and the next day, cell culture medium was changed prior to stimulation to reduce the background related to constitutive IL-8 synthesis. Then, cells were stimulated for 14–18 h with a dilution series of AuNPs, AuNPs-immobilized PDL192 (three batches), and Flag-TWEAK with and without crosslinking with the anti-Flag antibody M2. Crosslinking of Flag-TWEAK confers membrane TWEAK-like activity (Roos *et al.*, 2010) (A). Cells were likewise challenged with the anti-F14 antibody PDL192 in the presence of HEK293 cells transfected with a FcγR2-encoding expression plasmid or empty vector (EV) as a control. The HT1080 variants were also challenged with HEK293 cells transfected with a membrane-TWEAK encoding expression plasmid (B). The next day, cell supernatants were assayed for IL-8 production using ELISA. Please note, the concentration of the AuNPs refer to the nanoparticles and not to the amount of conjugated antibody.

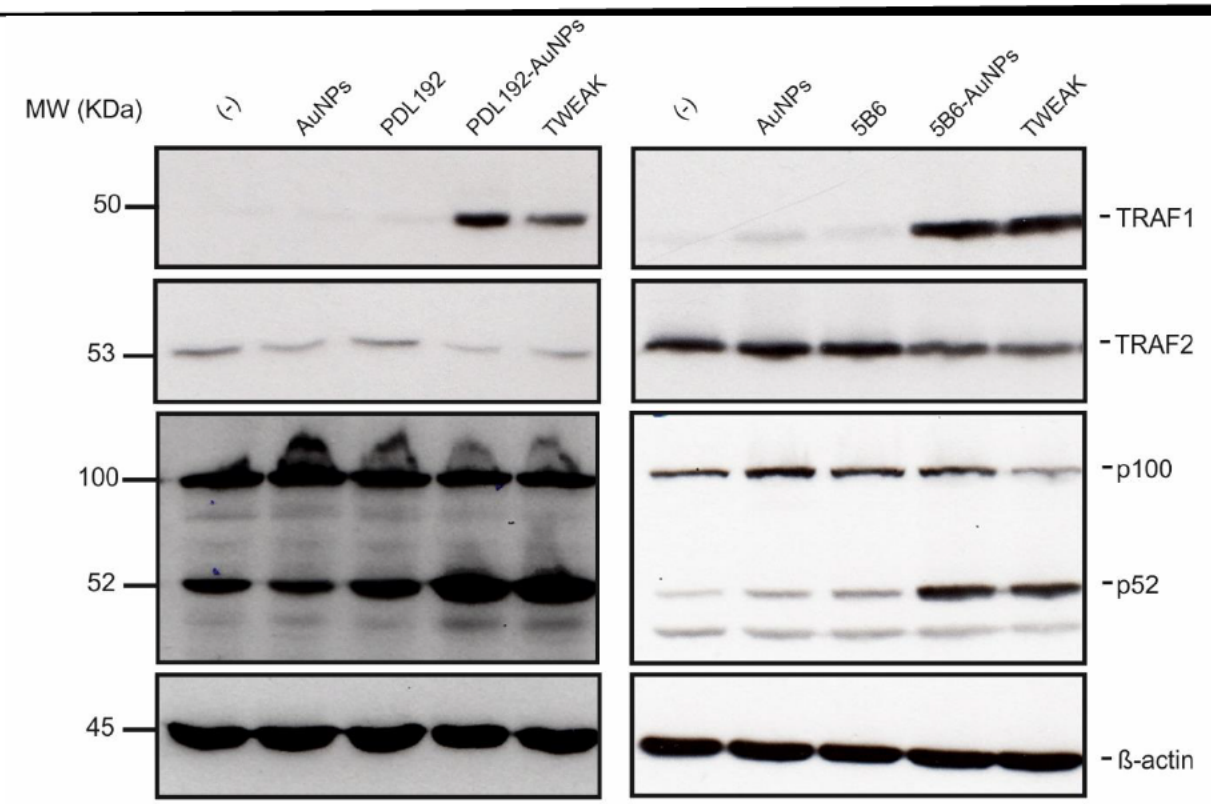


**Figure 14: AuNPs-immobilized anti-Fn14 antibodies (PDL192- and 5B6-AuNPs) efficiently trigger p100 processing and induce TRAF1 expression and weak TRAF2 depletion in a similar fashion to sTWEAK.**

HT1080 cells (1x$10^6$/well) were seeded in 6-well plates and treated the next day with AuNPs (1 mg/mL), PDL192-AuNPs (1 mg/mL), 5B6-AuNPs (2 mg/mL), PDL192 (400 ng/mL), and 5B6 (400 ng/mL) for 16–18 h. Treatment with Flag-TWEAK (200 ng/mL) served as a positive control. Finally, whole cell lysates were prepared and subjected to western blot analysis to detect TRAF1 induction, TRAF2 degradation, and p100 to p52 processing. Please note, the concentration values of the AuNPs refer to the nanoparticles and not to the amount of conjugated antibody.

Like p100 processing, the necroptosis-enhancing activity of Fn14 results from its ability to deplete cytoplasmic TRAF2 and so making it less available for the use of other receptors, e.g., TNFR1, which uses TRAF2 to antagonize necroptosis (Wicovsky *et al.*, 2009; Grabinger *et al.*, 2017). Indeed, AuNP-immobilized anti-Fn14 antibodies but not control AuNPs enhanced TNF-induced necroptosis in FADD-deficient HeLa-RIPK3 cells (Füllsack *et al.*,

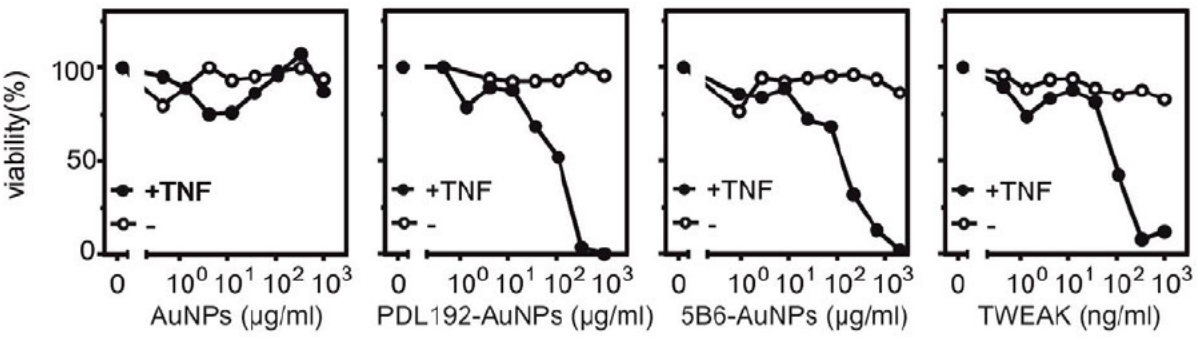


**Figure 15: AuNP-immobilized anti-Fn14 antibodies but not control AuNPs enhanced TNF-induced necroptosis in FADD-deficient HeLa-RIPK3 cells.**

Hela-RIP3-$FADD_{KO}$ cells (20 .$10^3$/well) were seeded in 96-well tissue plates. The next day, cells were treated in the presence or absence of TNF (1 ng/mL) with the indicated concentrations of AuNP-immobilized PDL192, AuNP-immobilized 5B6, AuNPs, or Flag-TWEAK to trigger TNF-induced cell death. Cell viability was determined after 18 h via crystal violet staining. Please note, the concentration values of the AuNPs refer to the nanoparticles and not to the amount of conjugated antibody.

2019) as well as soluble TWEAK (**Figure 15**). In sum, the analyses of Fn14 signaling activities suggest that AuNP-immobilized anti-Fn14 antibodies mimic membrane-bound TWEAK and can therefore be used as Fn14 agonists.

### 4.5. Immobilizing Conventional Antibodies Targeting Different TNFRs on AuNPs Improve their Agonism in a similar fashion to Cell-anchored Antibodies or Membrane-bound Ligand

Soluble ligand trimers and bivalent antibodies can bind and efficiently activate a subgroup of

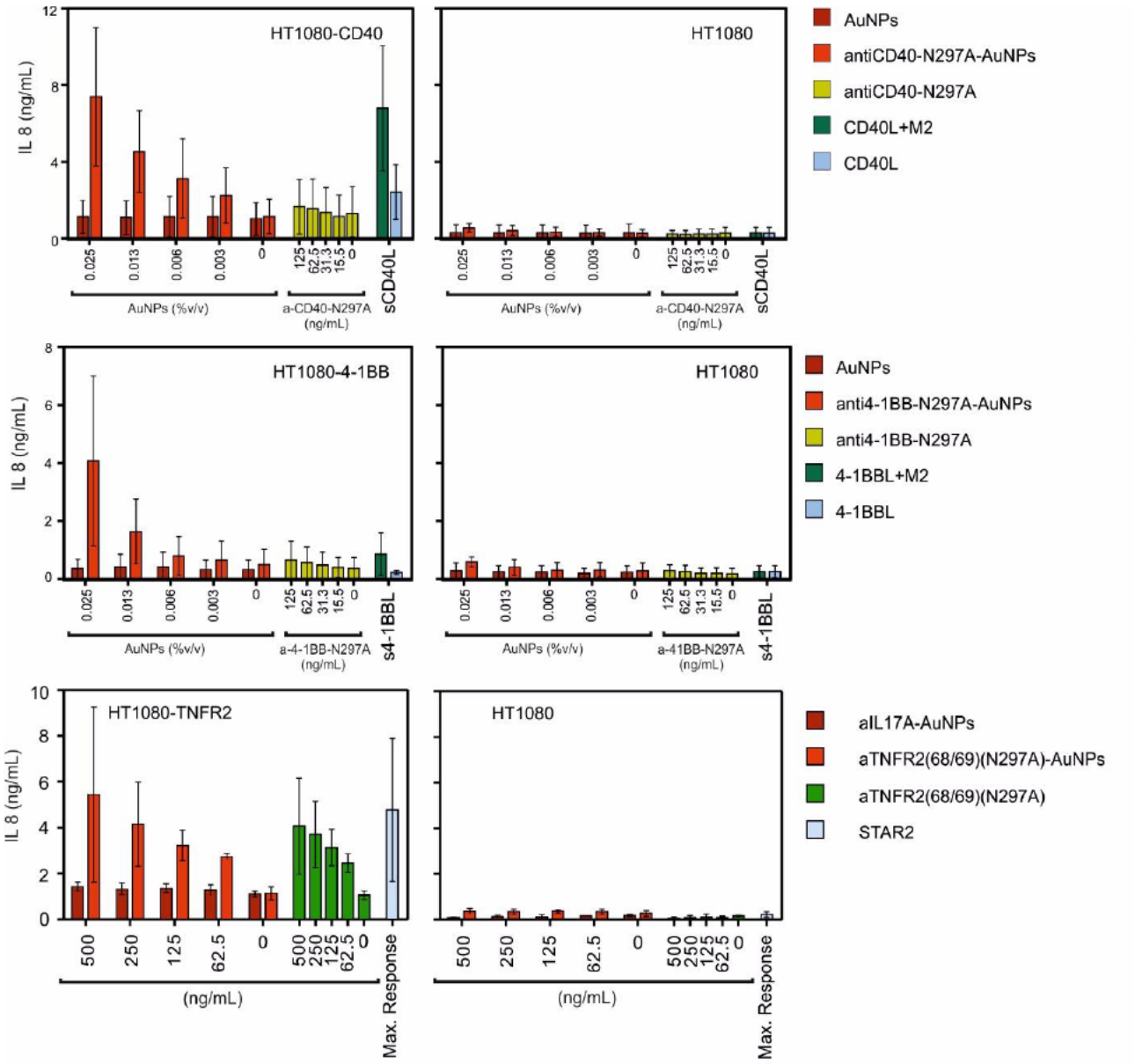


**Figure 16: AuNPs-immobilized with antibodies against proinflammatory TNFRs display membrane-bound ligand-like activity.**

HT1080-CD40 or HT1080cells (20 × $10^3$/well) were seeded in 96-well plates, and the next day, cell culture medium was changed prior to stimulation to reduce the background related to constitutive IL8 synthesis. Then, cells were stimulated for 14–18 h with a dilution series of AuNPs, AuNPs-immobilized antiCD40-N297A (G28.5), antiCD40-N297A (G28.5), and Flag-CD40L 200 ng/mL with and without crosslinking with the anti-Flag antibody (M2) 1 mg/mL. Crosslinking of Flag-CD40L confers membrane CD40L-like activity. The next day, cell supernatants were assayed for IL8 production using ELISA. (These data represent four independent experiments).

TNFRSF receptors (TNFRs), whereas a second subgroup of TNFRs can be efficiently stimulated only by binding to the oligomerized or plasma membrane-bound form of these ligand and antibodies. The second subgroup of TNFRs includes among other CD40, 41BB, OX40, CD27 and TNFR2 (Wajant, 2015).

We investigated the role of coupling IgG antibodies targeting TNFR receptors of the second subgroup such as CD40, 41BB or TNFR2 to gold nanoparticles to prove whether this regularly provides these antibodies with agonistic activity similar to FcγR-bound antibodies or membrane-bound ligands mode of action. To achieve that, we immobilize the IgG1(N297A) variant of anti-CD40, anti-41BB or anti-TNFR2 antibody on gold nanoparticles. The mutation N297A prevents the antibody to be bound by FcγRs. The agonistic activity of the AuNPs-immobilized anti-TNFR IgG antibodies resembled the activity of the corresponding oligomerized soluble ligand molecules by triggering the IL8-inducing signaling pathway in HT1080 cells stably expressing the TNFR of interest (HT1080-CD40, HT1080-41BB or HT1080-TNFR2). **Figure 16** clearly shows the qualitatively similar effect of AuNP-immobilized IgG antibodies and the anti-Flag oligomerized-soluble CD40L/ -soluble 41BBL molecules or STAR2, a sTNF oligomeric fusion protein, in triggering IL-8 production (a hallmark of the classical NFκB pathway), whereas the soluble IgG antibodies have not or poorly activated the studied signaling pathway. In the control group of the wild type HT1080 cells, there was no increased IL-8 production confirming the CD40, 41BB or TNFR2 specificity.

### 4.6. Gold Nanoparticles-immobilized anti-TNF IgG Antibody Embedded in Hydrogel blocks TNF locally

According to what has been demonstrated previously, the coupling of antibodies to gold nanoparticles did not interfere with their ability to bind the corresponding receptors. Based on this fact, we exploited the gold nanoparticles also as a platform to immobilize monoclonal IgG antibodies blocking cytokines such as TNF and IL1α. Hydrogel like Gelatin-methacryloyl (GelMa) has been utilized as a biocompatible and 3D printable material to deliver biomolecules locally through embedding live cells or functional proteins (Schloss, Williams and Regan, 2016). The release rate of proteins from such 3D printed tissue has been still considered as a challenge to create a sustainable biomaterial system. We investigated if the embedding of gold nanoparticles-immobilized antibody in the hydrogel can help to control the release rate of the biomolecule and to equip the system also with a localized cytokine inhibitory capacity.

### 4.6.1. Gold Nanoparticles can be Retained in Crosslinked GelMa A or only Diffuse with Very slow-release Rate

To characterize the ability of GelMa A to retain the gold nanoparticles-immobilized antibody for a longer time than the uncoupled antibodies, we evaluated the released amount of gold nanoparticles from the gel in the supernatant and compared it with the unreleased rest in the gel through the analysis by inductively coupled plasma mass spectrometry (ICP-MS).

To perform this analysis, a selected amount of the GelMa A was mixed with anti-TNFR2-AuNPs as a model with cells, either the variant expressing the relevant receptor (HT1080-TNFR2) or the wild type of cells (HT1080), or without cells. The three previous mixtures were crosslinked, in a shape of a disc in 96 wells plate, by exposing to ultraviolet light for 30

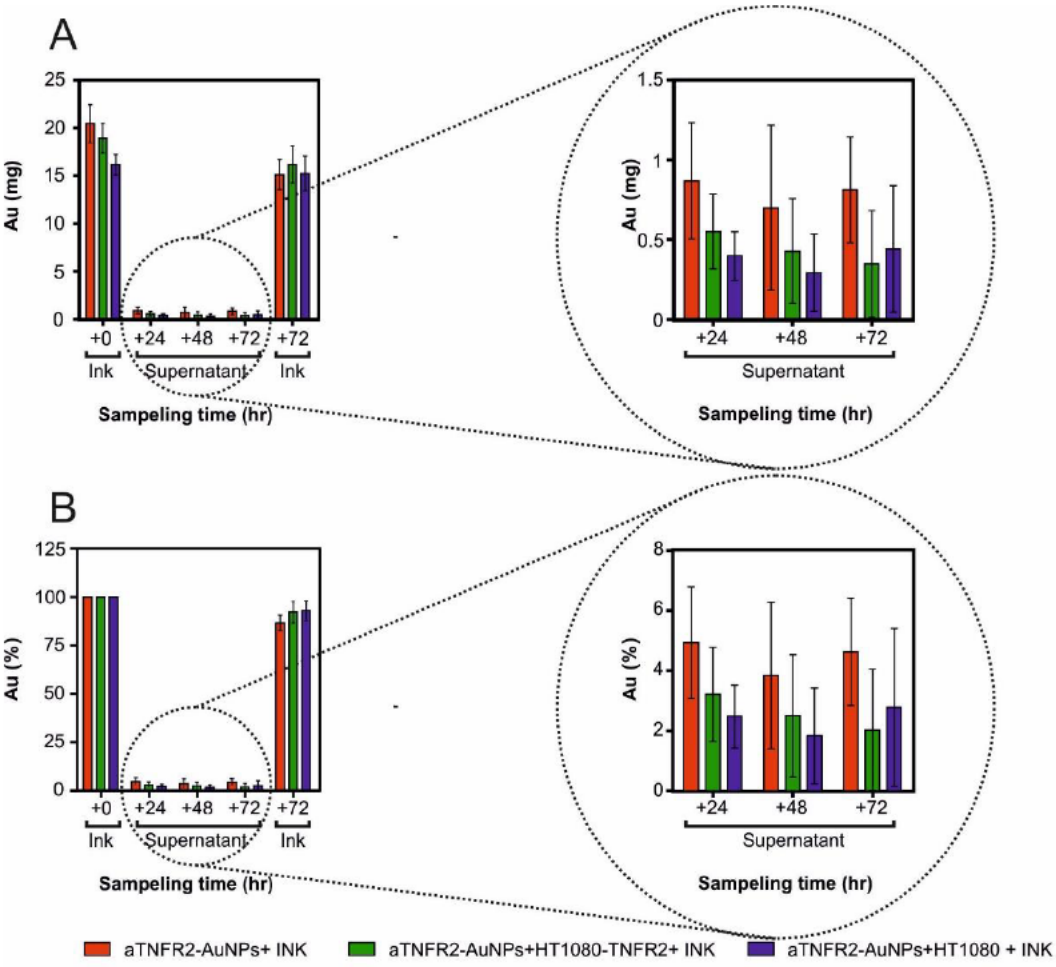


**Figure 17: Characterization of the release of AuNPs from GelMa A.**

A volume of anti-TNFR2-(68/69)-N297A-AuNPs was mixed with a volume of GelMa (Final concentration of particles is 0.1% (V/V) with final volume of 100 µL) and with $5.10^5$ HT1080/HT1080-TNFR2 or without, then the mixture was exposed to UV for 30 seconds for crosslinking and then incubated in CaCl2 to ensure the crosslinking for 5 min then washed with PBS and then the PBS was removed, finally the groups were incubated in 150 mL RPMI medium 10% FBS in 96 wells plate for 24 h, then the medium has been replaced with fresh medium for 24 h and with another fresh medium for another 24 h. The ICP-MS measurement of Au, according to the absolute mass (mg) A or according to the percentage (%) B, were performed on the ink after total incubation for +72h and the supernatant (medium RPMI 10 % FBS) after each replacement +24 h, +48 h and +72 h. As a control, another group of discs of the same three mixtures were prepared simultaneously, crosslinked, and stored for the measurement with the previous group. (These data represent two independent experiments, in each three technical replicates were performed)

seconds and incubation with calcium chloride for 5 minutes. The three discs were then incubated in a fresh RPMI 1640 medium with 10% FCS for 24 h, then the medium has been replaced with fresh medium for 24 h and with another fresh medium for another 24 hr. All replaced supernatants were collected according to the course of the time and analyzed for the absolute mass of Au after 0, 24, 48 and 72 h of the incubation. Additionally, we measured the unreleased rest of the Au mass in the ink after the incubation for 72 h in the medium by dissolving the gel and the gold nanoparticles using mixture of hydrochloric acid nitric acid (Aqua regia) overnight. To evaluate the total amount of Au retained in the gel before the incubation, additional group of the discs were prepared in parallel with the previous group, crosslinked and stored to measure the Au mass without incubation in the medium by dissolving the discs as previously mentioned.

Only minority amount of gold nanoparticles has been released from the gel through the incubation time to the surrounding medium as demonstrated in **Figure 17**, the presence of cells has reduced interestingly the release rate of gold nanoparticles in comparison to the cell free mixture.

All in all, gold nanoparticles can be reserved for days in the crosslinked gel, which is incubated in RPMI medium, what can be exploited to control and reduce the release rate of the functional proteins by coupling with gold nanoparticles to be utilized as sustainable local functioning particles.

### 4.6.2. Gold Nanoparticles-immobilized Antibodies Embedded in GelMa A Locally Restrict the Activity of Inflammatory Cytokines

Tumor necrosis factor alpha (TNFα) has been shown to be involved in the inflammatory reaction as the most important amplifying factor. TNFα binds to two different receptors, TNFR1 and TNFR2 which leads to stimulation of variety cellular responses, including cell

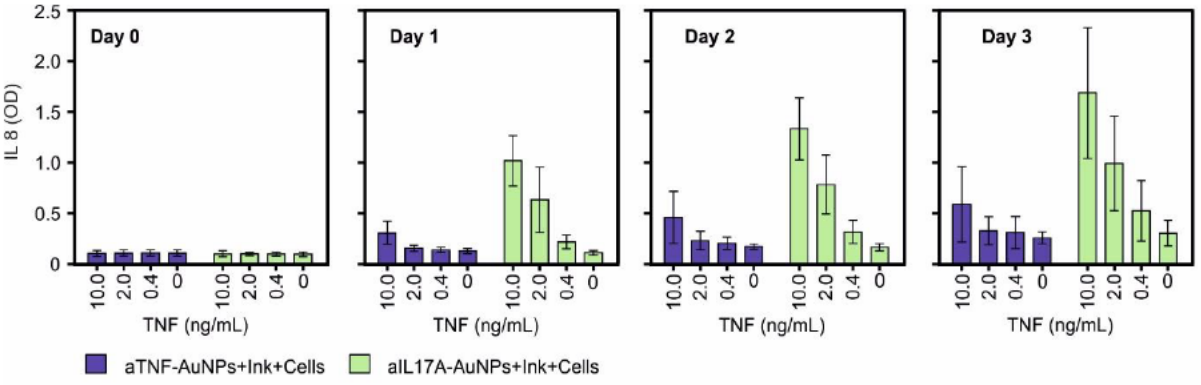


**Figure 18: Characterization of the blocking effect of anti-TNF-AuNPs in GelMa A.**

1 mL of GelMa A ink was mixed with $5.10^6$ HT-1080 cells, then divided to two parts, one part was mixed with anti-TNF-AuNPs and the other one with anti-IL17A-AuNPs (final concentration of particles 0.1% (V/V)). Each group was crosslinked with UV and $CaCl_2$, washed with PBS followed by RPMI medium) FBS 10 % and challenged with a dilution series of TNF. Samples of supernatants were collected prior to stimulation (Day 0) and after 1, 2 and 3 days of stimulation, then the samples were assayed for IL 8 production using ELISA.

survival, differentiation, and proliferation. However, its excessive activity can be associated with various autoimmune diseases (Jang *et al.*, 2021). Adalimumab (Humira™, Abbott Pharmaceutical Inc.), a fully humanized antibody has been utilized effectively in treating several autoimmune diseases through its specific blocking effect of TNFα. Clinical data show serious infections and other adverse events related to the administration of TNF blocking (Li *et al.*, 2021).

Local blocking of TNFα can be considered as an effective way to overcome such complications. The retained gold nanoparticles in the crosslinked gel can be utilized as local TNF blocker. To confirm that, a group of mixtures of AuNPs-immobilized anti-TNF antibody with HT1080 cells and GelMa A was prepared and crosslinked with UV and incubated in $CaCl_2$ as previously performed. Similarly, another group of mixtures was prepared but by substituting the particles with control variant (anti-IL17A-AuNPs). Both groups were challenged simultaneously with a dilution series of TNF for three days. Samples of the surrounding medium were collected prior to stimulation and after 1 day, 2 days and 3 days. Then, they were assayed for IL-8 production using ELISA.

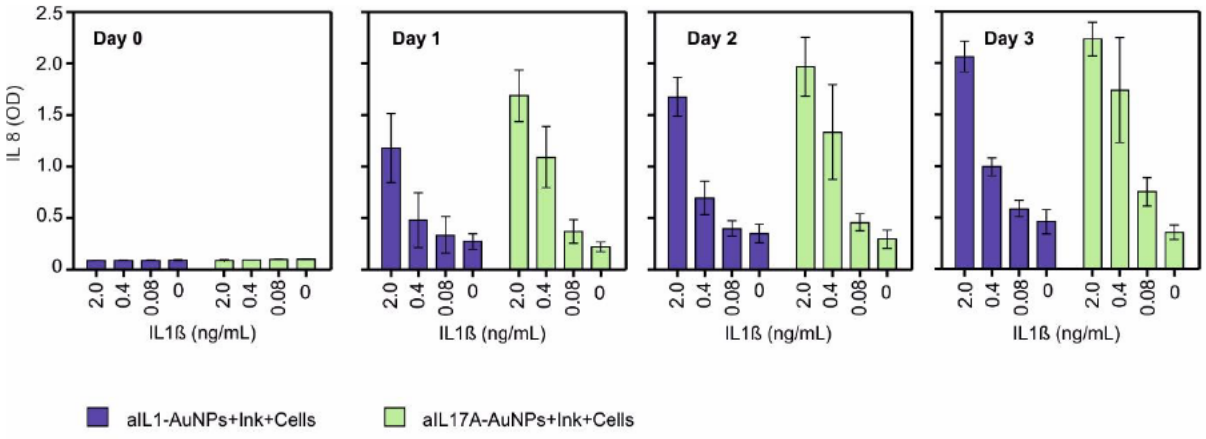


**Figure 19: Characterization of the blocking effect of anti-IL1-AuNPs in GelMa A.**

1 mL of GelMa A ink was mixed with $5.10^6$ HCT116-PIK3$_{mut}$ cells, then divided to two parts, one part was mixed with AuNPs-immobilized antiIL1 and the other one with AuNPs-immobilized antiIL17A (final concentration of particles: 0.1% (V/V)). Each group was crosslinked with UV and CaCl2, washed with PBS followed by RPMI medium, FBS 10 % and challenged with a dilution series of IL1ß. Samples of supernatants were collected prior to stimulation (Day 0) and after 1, 2 and 3 days of stimulation, then the samples were assayed for IL 8 production using ELISA.

Anti-TNF-AuNPs mixed with GelMa A were able to bind to the soluble TNF and prevent the stimulation of the TNFR1-expressing HT1080 which led to a poor or no production of IL-8 (a hallmark of the classical NFκB pathway) (**Figure 18**). Likewise, another antibody, anti-IL1 has been coupled with gold nanoparticles and mixed with GelMa A and the related receptor-expressing cells and crosslinked as aforementioned, then challenged with a dilution series of IL1ß. AuNPs-immobilized anti-IL1 antibody acted as antagonizing particles which reduced partly the stimulation of IL1R receptors-expressing HCT116-PIK3$_{mut}$ cells up to two days by 2 ng/mL of IL1ß and up to three days by 0.4 ng/mL of IL1ß (**Figure 19**). Higher inhibition effect

of IL1ß might be acquired by increasing the concentration of the particles or the coupled antagonizing antibody.

### 4.6.3. AuNP-immobilized Anti-TNF Antibodies but not Control AuNPs Blocks TNF-induced Necroptosis in FADD-deficient HeLa-RIPK3 Cells

Noteworthy, TNFα induces not only the proinflammatory signaling pathway, but also cell death either apoptosis or the program necrosis (necroptosis), through its ligation with TNFR1. The interaction of TNFR1 with TNFα results intracellularly in the recruitment of TRADD to the DD of TNFR1 triggering formation of complex IIc which induce RIPK3-mediated necroptosis and inflammation via the activation of its substrate mixed lineage kinase like (MLKL) (Jang *et al.*, 2021). Moreover, sensitizing the cells with tumor necrosis factor (TNF)-like weak inducer of apoptosis (TWEAK) can enhance both TNF-induced caspase-dependent apoptosis and TNF-triggered necrosis (Wicovsky *et al.*, 2009).

To characterize the blocking effect of gel-embedded anti-TNF-AuNPs also in hindering TNF-induced necroptosis, FADD-deficient HeLa-RIPK3 cells were investigated. Fas associated death domain (FADD) was shown to be involved in the apoptosis cascade blocking TNFR1-induced necroptosis. HeLa-RIP3-$FADD_{KO}$ cells were mixed with either anti-TNF-AuNPs or with anti-IL17A-AuNPs, then they were mixed with GelMa A ink, crosslinked by UV and CaCl2, washed with PBS followed by RPMI medium (FBS 10 %) and stimulated with a dilution series of TNF in the presence of a constant amount of soluble TWEAK. **Figure 20** demonstrates that anti-TNF-AuNPs gained the ability to block TNFR1-induced necroptosis which led to survival of cells. In sum, the previous findings suggest that gel-embedded AuNP-immobilized antibodies like anti-TNF-AuNPs or anti-IL1-AuNPs can be used as antagonizing molecules for local anti-inflammatory therapeutic use.

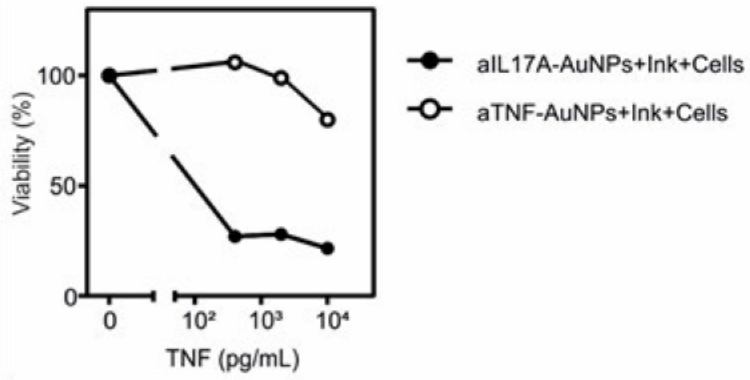


**Figure 20: AuNP-immobilized anti-TNF antibodies but not control AuNPs blocked locally TNF-induced necroptosis in FADD-deficient HeLa-RIPK3 cells.**

1 mL of GelMa A ink was mixed with $5.10^5$ HeLa-RIP3-$FADD_{KO}$ cells, then divided to two parts, one part was mixed with anti-TNF-immobilized AuNPs and the other one with antiIL17A-immobilized AuNPs (final concentration of particles is 0.1% (V/V)). Each group was crosslinked with UV and CaCl2, washed with PBS followed by RPMI medium) FBS 10 %) and challenged with a dilution series of TNF in the presence of TWEAK 200 ng/mL. Next day, the supernatants were assayed using MTT assay to characterize the viability of the cells after local blocking of the TNF through the anti-TNF-AuNPs mixed with the cells in the ink.

# 5. Discussion

## 5.1. Immobilizing anti-TNF receptors antibodies on AuNPs confer them with agonism

TNF receptors (TNFRs) have received significant attention in recent research for the development of new immune therapy strategies against various types of cancer. This is due to the abundant expression of TNF receptors on tumor cells and nonhematopoietic cells in the tumor microenvironment (Wajant, 2013; Beatty, Li and Long, 2017; Siegmund, Wagner and Wajant, 2022). Activation of these molecules triggers proinflammatory signaling pathways in the tumor microenvironment, leading to the recruitment of effector immune cells and impairing cancer cells.

Recent studies have found that free antibodies targeting subgroup of the TNFRSF receptors are largely inactive and only acquire membrane bound stimulatory mechanism after oligomerization using protein G or after anchoring to Fc receptors, thereby presenting the antibody in a pseudo membrane-bound form [5,15]. However, crosslinking by protein G or secondary antibodies, as well as FcR-anchoring, face obstacles and may lead to undesired aberrations. Additionally, anchoring to Fc receptors expressed on immune cells may induce their destruction, counteracting the aim to trigger immune stimulatory TNFRSF receptors. Furthermore, Fc receptors are exposed also on variety of undamaged cells, thus the activation of TNFRs in a far region from the tumor microenvironment leads to excessive activation of immune responses unleashing autoinflammatory responses as potential side effects (Scott, Wolchok and Old, 2012; Lang, Zaitseva and Wajant, 2022).

Our group has found that antibody targeting TNFRs can exhibit FcγR-independent agonism when fused with anchoring domains, allowing the immobilizing on specific cells. Moreover, selecting the targets of these domains directs the antibodies to specific tissues, preventing systemic off-target activation (Medler *et al.*, 2019).

Recently, a cell-free anchoring strategy has been investigated to overcome the inactivity of soluble TNF ligands. This strategy involves attaching the soluble ligands to nanostructures, such as silica core-shell beads, to mimic the membrane-bound mode of action (Bryde *et al.*, 2005). The covalent immobilization of proteins on nanostructures eliminates the need for additional anchoring domains. Numerous studies have shown also that conjugating antagonistic or agonistic antibodies with nanoparticles increases their activity compared to free antibodies. This approach also allows for the concentration of antibodies at the targeted site through the enhanced permeability and retention (EPR) effect, preventing systemic toxicity associated with the random distribution of free antibodies (Kosmides *et al.*, 2017; Zhang *et al.*, 2018). Moreover, loading biologics, such as checkpoint blockade therapeutics,

onto nanoparticles allows for dose reduction, reducing off-target side effects caused by high drug doses (Kosmides *et al.*, 2017).

Gold nanoparticles are highly attractive inorganic metallic particles with diverse biomedical applications. Spherical gold nanoparticles possess superior physicochemical and optoelectronic properties, such as a large surface-to-volume ratio, conductivity, and surface plasmon resonance, making them suitable for medical imaging as tag or contrast agents and for delivering various types of conjugates, including genes, chemicals, proteins, antibodies, or other targeting molecules for selective attacking of cancer cell. Furthermore, The functionalization of gold nanoparticles with compounds promotes their biocompatibility and long-term interaction with human tissues (Dreaden *et al.*, 2012; Zhang, 2015; Moustakas *et al.*, 2022).

Based on these facts, it is tempting to speculate that the attachment of gold nanoparticles to anti-TNF receptors antibodies is the decisive factor conferring agonistic activity. Our results suggest that conjugating monoclonal anti-TNFR antibodies to gold nanoparticles can be exploited to uncover their latent agonism, particularly for immunotherapeutic applications (**Figure 13**, **Figure 16**) (Aido *et al.*, 2021). Furthermore, the chemical conjugation method used did not show adverse consequences on the functionality of the attached antibodies and ensured strong and stable covalent coupling with carboxyl-modified AuNPs (**Figure 11**).
This approach demonstrates promising applications of nanocomposites with anti-tumor antibodies, allowing precise targeting of tumor tissues and preventing systemic side effects.

It is noteworthy that the size of the final construct was taken into consideration during the synthesis of the gold nanoparticles and the subsequent conjugation process. Preferably, the size should be in the range of 100-200 nm due to several reasons:

1. This size range has demonstrated optimal and selective cellular uptake and accumulation in tumors, as it can passively target the leaky vasculature of solid tumors through the enhanced permeability and retention (EPR) effect (Kosmides *et al.*, 2017; Zhang *et al.*, 2018).
2. Within this size range, the plasmon resonance peak in the near-infrared (NIR) region can be exhibited. This allows for the utility of the particles in photoacoustic imaging and efficient photothermal therapy in hyperthermia-based cancer therapy (Dreaden *et al.*, 2012).
3. Particles within this size range have shown optimal clearance from the body via the kidneys, resulting in minimal toxicity and immunogenicity compared to larger particles (Longmire, Choyke and Kobayashi, 2008).

Our model has been investigated *in Vitro* on individual cell lines. However, the success of this construct in an *in Vivo* system may face various hindrances and challenges. These include the accumulation or aggregation of particles in specific organs, the coupling of particles with molecules in the bloodstream leading to the blocking of attached antibodies, and the interaction of attached antibodies with undesired cells exposing the related receptors. Additionally, the targeted receptors may be expressed on other cells, albeit with lower concentration. To improve the prevention of systemic activity, an additional procedure of encapsulating the antibody-immobilized AuNPs may be required. This encapsulation can be performed using a specific polymer complex responsive to the tumor microenvironment, such as low pH or high levels of reactive oxygen species (ROS), which are characteristic features of many solid tumors. Consequently, the antibodies-immobilized AuNPs will be released only in close proximity to the targeted sites [109].

In future perspectives of our findings, one can also benefit from attaching anti-TNF receptor antibodies to gold nanoparticles to promote anti-tumor treatment through a combination with selective thermal stimulation of the targeted cancer cells upon addressing the attached antibodies (Dreaden *et al.*, 2012). Moreover, coupling different antibodies targeting two or more TNF receptor types, or simultaneously blocking the inhibitory checkpoint PD-L1 signal and stimulating T cells, has shown a promising combined immunotherapy approach for many tumor models (Kosmides *et al.*, 2017; Mi *et al.*, 2018; Zhang *et al.*, 2018).

Overall, a combined anti-tumor treatment involving thermal therapy by gold nanoparticles, in addition to encapsulation of this system, may present an innovative approach to developing more effective and targeted cancer therapies. Additionally, the encapsulation approach will combine the advantages of targeted drug delivery with the responsiveness of polymer-based drug delivery systems, revolutionizing cancer therapy and improving patient outcomes.

### 5.2. The incorporation of antibodies-immobilized AuNPs with photo-crosslinked hydrogel can be applied as novel local anti-inflammatory therapeutic.

Photo-crosslinked hydrogels, such as methacrylate-modified gelatin (GelMA) and hyaluronic acid (HAMA), have been extensively involved in various applications as tissue engineering scaffolds and drug delivery vehicles (Langer and Vacanti, 1993; Khademhosseini and Langer, 2016). Advances in technology, such as novel automation systems and computer-aided design (CAD), have revolutionized the fabrication of 3D cell-containing constructs. These constructs are not limited to regenerative medicine but also serve as 3D in vitro models for studying disease mechanisms and drug screening (Pati, Gantelius and Svahn, 2016). Moreover, biofabrication materials like GelMA are enriched with biological molecules, including growth factors, necessary for cell differentiation and (Schloss, Williams and Regan, 2016; Zhang *et al.*, 2016). This allows the embedding of live cells in printed complex

structures, referred to as bioinks, which can act as sustainable reactors for producing critical biologicals in an environment close to that of natural tissues.

The incorporation of nanoparticles within 3D printed constructs has shown promising potential for therapeutic and medical imaging applications (Li *et al.*, 2020, 2022). Additionally, conjugates-attached nanoparticles can play a critical role in regulating the growth and differentiation processes of embedded cells.

Based on these considerations, we aimed to exploit our established system of anti-TNF receptors-immobilized gold nanoparticles (AuNPs) and apply them as inhibitory molecules by embedding them in a bioink containing the cells of interest. As a first step, we characterized the retention of gold nanoparticles in the crosslinked GelMa A. Our finding shows that the gold nanoparticles only diffuse with very slow-release rate (**Figure 17**). These results exhibit the advantage of embedding biologicals-conjugated AuNPs in comparation to integration only the free biologicals, which can be released from the bioink in a short window of time.

Next, we coupled two types of monoclonal therapeutic antibodies targeting TNFα, Adalimumab, or IL1β, Ilaris® (Canakinumab) with AuNPs, which are widely used in treatment of autoinflammatory diseases. Subsequently, the antibody-immobilized AuNPs were mixed with GelMa A and the respective cells expressing the targeted receptors. As depicted in **Figure 18**, **Figure 19** and **Figure 20**, our results obviously demonstrated that these constructs antagonized the added cytokines up to three days in the case of TNFα and up to two days IL1ß. These experiments served as a proof of concept. However, a higher effect can be acquired upon the increase of the amount of attached blocking antibodies. Additionally, the ratio of the added components needs to be adjusted to ensure the stability and integrity of the crosslinked gel.

This approach presents a promising strategy for creating a sustainable local inhibitory system, which can be employed as antagonizing molecules for local anti-inflammatory therapeutics. The localization of blocking antibodies prevents excessive systemic targeting effects, thus reducing the risk of serious infections and other adverse events associated with the administration of free soluble TNF blockers in the bloodstream (Li *et al.*, 2021).

## 6. Summary

Gold nanoparticles of diameter ca. 60 nm have been synthesized based on Turkevich and Frens protocols. We have demonstrated that the carboxyl-modified gold nanoparticles can be coupled covalently with antibodies (Ab) of interest using the EDC/NHS coupling procedure. Binding studies with Ab-grafted AuNPs and GpL fusion proteins proved that conjugation of AuNPs with antibodies enables immobilization of antibodies with preservation of a significant antigen binding capacity. More importantly, our findings showed that the conjugation of types of anti-TNF receptors antibodies such as anti-Fn14 antibodies (PDL192 and 5B6) (Aido *et al.*, 2021), anti-CD40, anti-4-1BB and anti-TNFR2 with gold nanoparticles confers them with potent agonism. Thus, our results suggest that AuNPs can be utilized as a platform to immobilize anti-TNFR antibodies which, on the one hand, helps to enhance their agonistic activity in comparison to "free" inactive antibodies by mimicking the effect of cell-anchored antibodies or membrane-bound TNF ligands and, on the other hand, allows to develop new generations of drug delivery systems. These constructs are characterized with their biocompatibility and their tunable synthesis process.

In a further work part, we combined the benefits of the established system of Ab-AuNPs with materials used widely in the modern biofabrication approaches such as the photo-crosslinked hydrogels, methacrylate-modified gelatin (GelMA), combined with embedded variants of human cell lines. The acquired results demonstrated clearly that the attaching of proteins like antibodies to gold nanoparticles might reduce their release rate from the crosslinked hydrogels upon the very low diffusion of gold nanoparticles from the solid constructs to the surrounding medium yielding long-term local functioning proteins-attached particles. Moreover, our finding suggests that hydrogel-embedded AuNP-immobilized antibodies, e.g. anti-TNFα-AuNPs or anti-IL1-AuNPs enable local inhibitory functions,

To sum up, our results demonstrate that AuNPs can act as a platform to attach anti-TNFR antibodies to enhance their agonistic activity by resembling the output of cell-anchoring or membrane bounding. Gold nanoparticles are considered, thus, as promising tool to develop the next generation of drug delivery systems, which may contribute to cancer therapy. On top of that, the embedding of anti-inflammatory-AuNPs in the biofabricated hydrogel presents new innovative strategy of the treatment of autoinflammatory diseases.

## 7. Zusammenfassung

Gold-Nanopartikel mit einem Durchmesser von ca. 60 nm wurden auf Basis der Turkevich- und Frens-Protokolle synthetisiert. Bindungsstudien mit Ab-verankerten AuNPs und GpL-Fusionsproteinen haben gezeigt, dass die Konjugation von AuNPs mit Antikörpern die Immobilisierung von Antikörpern mit Erhaltung einer signifikanten Antigenbindungs-Kapazität ermöglicht. Noch wichtiger ist, dass unsere Ergebnisse zeigen, dass die Konjugation von Typen von Antikörpern gegen TNFRs wie anti-Fn14-Antikörper (PDL192 und 5B6), anti-CD40, anti-4-1BB und anti-TNFR2 mit Gold-Nanopartikeln ihnen eine starke agonistische Wirkung verleiht. Unsere Ergebnisse legen nahe, dass AuNPs als Plattform genutzt werden können, um Antikörper gegen TNFR zu immobilisieren, was einerseits dazu beiträgt, ihre agonistische Aktivität im Vergleich zu "freien" inaktiven Antikörpern zu erhöhen, indem sie die Wirkung von zellgebundenen Antikörpern oder membranverankerten TNF-Liganden nachahmen und andererseits die Entwicklung neuer Generationen von Wirkstoffabgabe Systemen ermöglicht. Diese Konstrukte zeichnen sich durch ihre Biokompatibilität und ihren einstellbaren Syntheseprozess aus.

In einem weiteren Teil der Arbeit haben wir die Vorteile des etablierten Systems von Ab-AuNPs mit Materialien kombiniert, die in modernen Biofabrikationsansätzen weit verbreitet sind, nämlich Hydrogele, z.b. methacrylatmodifiziertes Gelatine (GelMA), kombiniert mit eingebetteten Varianten von menschlichen Zelllinien. Die erzielten Ergebnisse zeigten deutlich, dass die Anbindung von Proteinen wie Antikörpern an Gold-Nanopartikel ihre Freisetzung aus den vernetzten Hydrogelen reduzieren könnte, da die Diffusion von Gold-Nanopartikeln aus den festen Konstrukten in das umgebende Medium sehr gering ist und so langfristig Konstrukte mit lokalem Proteine load - erzeugt werden können. Darüber hinaus legt unser Befund nahe, dass in das Hydrogel eingebettete AuNP-immobilisierte Antikörper wie Anti-TNFα-AuNPs oder Anti-IL1-AuNPs eine lokal Immunsuppression erlauben. Diese können als vielversprechende Ansätze betrachtet werden, um verschiedene Arten von Autoimmunerkrankungen zu behandeln.

Zusammenfassend zeigen unsere Ergebnisse, dass AuNPs als Plattform dienen können, um Anti-TNFR-Antikörper anzubinden und ihre agonistische Aktivität zu erhöhen. Goldnanopartikel werden daher als vielversprechendes Werkzeug zur Entwicklung der nächsten Generation von Wirkstofftransportsystemen angesehen, die zur Krebstherapie beitragen können. Darüber hinaus stellt die Einbettung von entzündungshemmenden-AuNPs in das biofabrizierte Hydrogel eine neue innovative Strategie für die Behandlung von autoinflammatorischen Erkrankungen dar.

## 8. References


Abbate, A. *et al.* (2010) 'Interleukin-1 blockade with anakinra to prevent adverse cardiac remodeling after acute myocardial infarction (Virginia Commonwealth University Anakinra Remodeling Trial [VCU-ART] Pilot study)', *The American journal of cardiology*. Am J Cardiol, 105(10). doi: 10.1016/J.AMJCARD.2009.12.059.

Aggarwal, B. B. (2003) 'Signalling pathways of the TNF superfamily: A double-edged sword', *Nature Reviews Immunology*. Nature Publishing Group, 3(9), pp. 745–756. doi: 10.1038/NRI1184.

Aido, A. *et al.* (2021) 'Anti-Fn14 Antibody-Conjugated Nanoparticles Display Membrane TWEAK-Like Agonism', *Pharmaceutics*. Pharmaceutics, 13(7). doi: 10.3390/PHARMACEUTICS13071072.

Aksentijevich, I. *et al.* (2002) 'De novo CIAS1 mutations, cytokine activation, and evidence for genetic heterogeneity in patients with neonatal-onset multisystem inflammatory disease (NOMID): A new member of the expanding family of pyrin-associated autoinflammatory diseases', *Arthritis and Rheumatism*, 46(12), pp. 3340–3348. doi: 10.1002/ART.10688.

Amendola, V. *et al.* (2017) 'Surface plasmon resonance in gold nanoparticles: A review', *Journal of Physics Condensed Matter*. Institute of Physics Publishing, p. 203002. doi: 10.1088/1361-648X/aa60f3.

Ashkenazi, A. and Dixit, V. M. (1998) 'Death receptors: Signaling and modulation', *Science*. American Association for the Advancement of Science, pp. 1305–1308. doi: 10.1126/science.281.5381.1305.

Bajor, D. L. *et al.* (2018) 'Long-term outcomes of a phase I study of agonist CD40 antibody and CTLA-4 blockade in patients with metastatic melanoma', *Oncoimmunology*. Oncoimmunology, 7(10). doi: 10.1080/2162402X.2018.1468956.

Bartkowiak, T. and Curran, M. A. (2015) '4-1BB Agonists: Multi-Potent Potentiators of Tumor Immunity', *Frontiers in Oncology*. Frontiers Media SA, 5(JUN), p. 1. doi: 10.3389/FONC.2015.00117.

Beatty, G. L., Li, Y. and Long, K. B. (2017) 'Cancer immunotherapy: activating innate and adaptive immunity through CD40 agonists', *Expert review of anticancer therapy*. Expert Rev Anticancer Ther, 17(2), pp. 175–186. doi: 10.1080/14737140.2017.1270208.

De Benedetti, F. *et al.* (2018) 'Canakinumab for the Treatment of Autoinflammatory Recurrent Fever Syndromes', *The New England journal of medicine*. N Engl J Med, 378(20), pp. 1908–1919. doi: 10.1056/NEJMOA1706314.

Beutler, B. A., Milsark, I. W. and Cerami, A. (1985) 'Cachectin/tumor necrosis factor: production, distribution, and metabolic fate in vivo.', *Journal of immunology (Baltimore, Md. : 1950)*. United States, 135(6), pp. 3972–3977.

Beutler, B. and Bazzoni, F. (1998) 'TNF, apoptosis and autoimmunity: A common thread?', *Blood Cells, Molecules and Diseases*. Academic Press Inc., 24(2), pp. 216–230. doi: 10.1006/bcmd.1998.0187.

Bodmer, J. *et al.* (2002) 'The molecular architecture of the TNF superfamily', 27(1), pp. 19–26.

Brown, S. A. N. *et al.* (2003) 'The Fn14 cytoplasmic tail binds tumour-necrosis-factor-receptor-associated factors 1, 2, 3 and 5 and mediates nuclear factor-kappaB activation', *The Biochemical journal*. Biochem J, 371(Pt 2), pp. 395–403. doi: 10.1042/BJ20021730.

Bryde, S. *et al.* (2005) 'Tumor Necrosis Factor (TNF)-Functionalized Nanostructured Particles for the Stimulation of Membrane TNF-Specific Cell Responses', *Bioconjugate Chemistry*. American Chemical Society , 16(6), pp. 1459–1467. doi: 10.1021/BC0501810.

Buchbinder, E. I. and Desai, A. (2016) 'CTLA-4 and PD-1 Pathways: Similarities, Differences, and Implications of Their Inhibition', *American Journal of Clinical Oncology*. Wolters Kluwer Health, 39(1), p. 98. doi: 10.1097/COC.0000000000000239.

Carswell, E. A. *et al.* (1975) 'An endotoxin-induced serum factor that causes necrosis of tumors Immunology ':, 72(9), pp. 3666–3670.

Chan, F. K. M. *et al.* (2000) 'A domain in TNF receptors that mediates ligand-independent receptor assembty and signaling', *Science*, 288(5475), pp. 2351–2354. doi: 10.1126/science.288.5475.2351.

Chen, D. S. and Mellman, I. (2013) 'Oncology meets immunology: The cancer-immunity cycle', *Immunity*, 39(1), pp. 1–10. doi: 10.1016/J.IMMUNI.2013.07.012.

Craig Smith, M. A. and Farmh, T. (1994) *The TNF Receptor Superfamily of Cellular and Viral Proteins: Activation, &stimulation, and Death*, *Cell*.

Croft, M. (2009) 'The role of TNF superfamily members in T-cell function and diseases', *Nature reviews. Immunology*. Nat Rev Immunol, 9(4), pp. 271–285. doi: 10.1038/NRI2526.

Dinarello, C. A. (2011) 'Interleukin-1 in the pathogenesis and treatment of inflammatory diseases', *Blood*. Blood, 117(14), pp. 3720–3732. doi: 10.1182/BLOOD-2010-07-273417.

Dostert, C. *et al.* (2019) 'The TNF family of ligands and receptors: Communication modules in the immune system and beyond', *Physiological Reviews*. American Physiological Society, 99(1), pp. 115–160. doi: 10.1152/PHYSREV.00045.2017/ASSET/IMAGES/LARGE/Z9J0041828770007.JPEG.

Dreaden, E. C. *et al.* (2012) 'The golden age: gold nanoparticles for biomedicine', *Chemical Society Reviews*. The Royal Society of Chemistry, 41(7), pp. 2740–2779. doi: 10.1039/C1CS15237H.

Dzimitrowicz, A. *et al.* (2019) 'Preparation and characterization of gold nanoparticles prepared with aqueous extracts of Lamiaceae plants and the effect of follow-up treatment with atmospheric pressure glow microdischarge', *Arabian Journal of Chemistry*, 12(8), pp. 4118–4130. doi: 10.1016/j.arabjc.2016.04.004.

El-Sayed, I. H., Huang, X. and El-Sayed, M. A. (2005) 'Surface plasmon resonance scattering and absorption of anti-EGFR antibody conjugated gold nanoparticles in cancer diagnostics: Applications in oral cancer', *Nano Letters*, 5(5), pp. 829–834. doi: 10.1021/nl050074e.

Elgueta, R. *et al.* (2009) 'Molecular mechanism and function of CD40/CD40L engagement in the immune system', *Immunological Reviews*. NIH Public Access, 229(1), pp. 152–172. doi: 10.1111/j.1600-065X.2009.00782.x.

Etemadi, N. *et al.* (2013) 'Lymphotoxin α induces apoptosis, necroptosis and inflammatory signals with the same potency as tumour necrosis factor', *The FEBS journal*. FEBS J, 280(21), pp. 5283–5297. doi: 10.1111/FEBS.12419.

Falvo, J. V., Tsytsykova, A. V. and Goldfeld, A. E. (2010) 'Transcriptional Control of the TNF Gene', *Current Directions in Autoimmunity*. Karger Publishers, 11, pp. 27–60. doi: 10.1159/000289196.

Fathi-Achachelouei, M. *et al.* (2019) 'Use of Nanoparticles in Tissue Engineering and Regenerative Medicine', *Frontiers in Bioengineering and Biotechnology*. Frontiers, 7, p. 113. doi: 10.3389/FBIOE.2019.00113.

Faustman, D. L. and Davis, M. (2013) 'TNF Receptor 2 and Disease: Autoimmunity and Regenerative Medicine', *Frontiers in immunology*. Front Immunol, 4(DEC). doi: 10.3389/FIMMU.2013.00478.

Feng, S. L. Y. *et al.* (2000) 'The Fn14 immediate-early response gene is induced during liver regeneration and highly expressed in both human and murine hepatocellular carcinomas', *The American journal of pathology*. Am J Pathol, 156(4), pp. 1253–1261. doi: 10.1016/S0002-

9440(10)64996-6.

Feoktistova, M., Geserick, P. and Leverkus, M. (2016) 'Crystal Violet Assay for Determining Viability of Cultured Cells.', *Cold Spring Harbor protocols*. United States, 2016(4), p. pdb.prot087379. doi: 10.1101/pdb.prot087379.

Fesik, S. W. (2000) 'Insights into programmed cell through structural biology', *Cell*. Elsevier B.V., 103(2), pp. 273–282. doi: 10.1016/S0092-8674(00)00119-7.

FRENS, G. (1973) 'Controlled Nucleation for the Regulation of the Particle Size in Monodisperse Gold Suspensions', *Nature Physical Science*. Springer Nature, 241(105), pp. 20–22. doi: 10.1038/physci241020a0.

Fuertes, M. B. *et al.* (2011) 'Host type I IFN signals are required for antitumor CD8+ T cell responses through CD8α+ dendritic cells', *The Journal of Experimental Medicine*. The Rockefeller University Press, 208(10), p. 2005. doi: 10.1084/JEM.20101159.

Füllsack, S. *et al.* (2019) 'Redundant and receptor-specific activities of TRADD, RIPK1 and FADD in death receptor signaling', *Cell Death and Disease*. Nature Publishing Group, 10(2), pp. 1–19. doi: 10.1038/s41419-019-1396-5.

Gattorno, M. *et al.* (2007) 'Pattern of interleukin-1beta secretion in response to lipopolysaccharide and ATP before and after interleukin-1 blockade in patients with CIAS1 mutations', *Arthritis and rheumatism*. Arthritis Rheum, 56(9), pp. 3138–3148. doi: 10.1002/ART.22842.

Goldbach-Mansky, R. (2011) 'Current status of understanding the pathogenesis and management of patients with NOMID/CINCA', *Current rheumatology reports*. Curr Rheumatol Rep, 13(2), pp. 123–131. doi: 10.1007/S11926-011-0165-Y.

Grabarek, Z. and Gergely, J. (1990) 'Zero-length crosslinking procedure with the use of active esters.', *Analytical biochemistry*. United States, 185(1), pp. 131–135. doi: 10.1016/0003-2697(90)90267-d.

Grabinger, T. *et al.* (2017) 'Inhibitor of Apoptosis Protein-1 Regulates Tumor Necrosis Factor-Mediated Destruction of Intestinal Epithelial Cells.', *Gastroenterology*. United States, 152(4), pp. 867–879. doi: 10.1053/j.gastro.2016.11.019.

Grell, M. *et al.* (1995) 'The transmembrane form of tumor necrosis factor is the prime activating ligand of the 80 kDa tumor necrosis factor receptor', *Cell*. Cell, 83(5), pp. 793–802. doi: 10.1016/0092-8674(95)90192-2.

Haiss, W. *et al.* (2007) 'Determination of size and concentration of gold nanoparticles from UV-Vis spectra', *Analytical Chemistry*, 79(11), pp. 4215–4221. doi: 10.1021/ac0702084.

Hehlgans, T. and Pfeffer, K. (2005) 'The intriguing biology of the tumour necrosis factor/tumour necrosis factor receptor superfamily: Players, rules and the games', *Immunology*, 115(1), pp. 1–20. doi: 10.1111/J.1365-2567.2005.02143.X.

Hsu, H., Xiong, J. and Goeddel, D. V. (1995) 'The TNF receptor 1-associated protein TRADD signals cell death and NF-kappa B activation', *Cell*. Cell, 81(4), pp. 495–504. doi: 10.1016/0092-8674(95)90070-5.

Idriss, H. T. and Naismith, J. H. (2000) 'TNFα and the TNF receptor superfamily: Structure-function relationship(s)', *Microscopy Research and Technique*, 50(3), pp. 184–195. doi: 10.1002/1097-0029(20000801)50:3<184::AID-JEMT2>3.0.CO;2-H.

Jang, D.-I. *et al.* (2021) 'The Role of Tumor Necrosis Factor Alpha (TNF-α) in Autoimmune Disease and Current TNF-α Inhibitors in Therapeutics.', *International journal of molecular sciences*. Switzerland, 22(5). doi: 10.3390/ijms22052719.

Jiang, Y. *et al.* (1999) 'Prevention of constitutive TNF receptor 1 signaling by silencer of death

domains.', *Science (New York, N.Y.)*, 283(5401), pp. 543–6. doi: 10.1126/science.283.5401.543.

Kelley, S. K. *et al.* (2001) *Preclinical Studies to Predict the Disposition of Apo2L/Tumor Necrosis Factor-Related Apoptosis-Inducing Ligand in Humans: Characterization of in Vivo Efficacy, Pharmacokinetics, and Safety*. Available at: http://jpet.aspetjournals.org (Accessed: 19 September 2019).

Khademhosseini, A. and Langer, R. (2016) 'A decade of progress in tissue engineering', *Nature protocols*. Nat Protoc, 11(10), pp. 1775–1781. doi: 10.1038/NPROT.2016.123.

Khlebtsov, B. N. and Khlebtsov, N. G. (2011) 'On the measurement of gold nanoparticle sizes by the dynamic light scattering method', *Colloid Journal*, 73(1), pp. 118–127. doi: 10.1134/S1061933X11010078.

Khubchandani, S., Czuczman, M. S. and Hernandez-Ilizaliturri, F. J. (2009) 'Dacetuzumab, a humanized mAb against CD40 for the treatment of hematological malignancies.', *Current opinion in investigational drugs (London, England : 2000)*. England, 10(6), pp. 579–587.

Kim, E. Y. *et al.* (2015) 'Recent advances in gold nanoparticle-based bioengineering applications', *Journal of Materials Chemistry B*. The Royal Society of Chemistry, 3(43), pp. 8433–8444. doi: 10.1039/C5TB01292A.

Kimling, J. *et al.* (2006) 'Turkevich method for gold nanoparticle synthesis revisited', *Journal of Physical Chemistry B*, 110(32), pp. 15700–15707. doi: 10.1021/jp061667w.

Kosmides, A. K. *et al.* (2017) 'Dual Targeting Nanoparticle Stimulates the Immune System To Inhibit Tumor Growth', *ACS nano*. ACS Nano, 11(6), pp. 5417–5429. doi: 10.1021/ACSNANO.6B08152.

Kums, J. *et al.* (2017) 'Quantitative analysis of cell surface antigen-antibody interaction using Gaussia princeps luciferase antibody fusion proteins.', *mAbs*, 9(3), pp. 506–520. doi: 10.1080/19420862.2016.1274844.

Lang, I., Zaitseva, O. and Wajant, H. (2022) 'FcγRs and Their Relevance for the Activity of Anti-CD40 Antibodies', *International Journal of Molecular Sciences*. MDPI, 23(21). doi: 10.3390/IJMS232112869.

Langer, R. and Vacanti, J. P. (1993) 'Tissue engineering', *Science (New York, N.Y.)*. Science, 260(5110), pp. 920–926. doi: 10.1126/SCIENCE.8493529.

Larsen, C. M. *et al.* (2007) 'Interleukin-1-receptor antagonist in type 2 diabetes mellitus', *The New England journal of medicine*. N Engl J Med, 356(15), pp. 1517–1526. doi: 10.1056/NEJMOA065213.

Li, H. *et al.* (2020) 'Advances in the application of gold nanoparticles in bone tissue engineering', *Journal of Biological Engineering*. BioMed Central, 14(1). doi: 10.1186/S13036-020-00236-3.

Li, J. *et al.* (2021) 'Risk of Adverse Events After Anti-TNF Treatment for Inflammatory Rheumatological Disease. A Meta-Analysis', *Frontiers in Pharmacology*. Frontiers Media S.A., 12, p. 3010. doi: 10.3389/FPHAR.2021.746396/BIBTEX.

Li, L. *et al.* (2022) 'Methacrylate-Modified Gold Nanoparticles Enable Non-Invasive Monitoring of Photocrosslinked Hydrogel Scaffolds', *bioRxiv*. Cold Spring Harbor Laboratory, p. 2022.01.26.477960. doi: 10.1101/2022.01.26.477960.

Longmire, M., Choyke, P. L. and Kobayashi, H. (2008) 'Clearance Properties of Nano-sized Particles and Molecules as Imaging Agents: Considerations and Caveats', *Nanomedicine (London, England)*. NIH Public Access, 3(5), p. 703. doi: 10.2217/17435889.3.5.703.

Luqman, M. *et al.* (2008) 'The antileukemia activity of a human anti-CD40 antagonist antibody, HCD122, on human chronic lymphocytic leukemia cells', *Blood*. Blood, 112(3), pp. 711–720. doi: 10.1182/BLOOD-2007-04-084756.

Macewan, D. J. (2002) 'REVIEW TNF ligands and receptors ± a matter of life and death'.

Mbanwi, A. N. and Watts, T. H. (2014) 'Costimulatory TNFR family members in control of viral infection: Outstanding questions', *Seminars in Immunology*. Academic Press, 26(3), pp. 210–219. doi: 10.1016/J.SMIM.2014.05.001.

Medler, J. *et al.* (2019) 'TNFRSF receptor-specific antibody fusion proteins with targeting controlled FcγR-independent agonistic activity', *Cell Death and Disease*. Springer US, 10(3). doi: 10.1038/s41419-019-1456-x.

Mehta, A. K., Gracias, D. T. and Croft, M. (2018) 'TNF activity and T cells', *Cytokine*. Academic Press, 101, pp. 14–18. doi: 10.1016/J.CYTO.2016.08.003.

Meighan-Mantha, R. L. *et al.* (1999) 'The mitogen-inducible Fn14 gene encodes a type I transmembrane protein that modulates fibroblast adhesion and migration', *Journal of Biological Chemistry*, 274(46), pp. 33166–33176. doi: 10.1074/JBC.274.46.33166.

Mi, Y. *et al.* (2018) 'A Dual Immunotherapy Nanoparticle Improves T-Cell Activation and Cancer Immunotherapy', *Advanced materials (Deerfield Beach, Fla.)*. Adv Mater, 30(25). doi: 10.1002/ADMA.201706098.

Moran, A. E., Kovacsovics-Bankowski, M. and Weinberg, A. D. (2013) 'The TNFRs OX40, 4-1BB, and CD40 as targets for cancer immunotherapy', *Current opinion in immunology*. Curr Opin Immunol, 25(2), pp. 230–237. doi: 10.1016/J.COI.2013.01.004.

Moroni, L. *et al.* (2018) 'Biofabrication: A Guide to Technology and Terminology', *Trends in Biotechnology*. Elsevier Ltd, 36(4), pp. 384–402. doi: 10.1016/J.TIBTECH.2017.10.015.

Motz, G. T. and Coukos, G. (2013) 'Deciphering and reversing tumor immune suppression', *Immunity*. Immunity, 39(1), pp. 61–73. doi: 10.1016/J.IMMUNI.2013.07.005.

Moustakas, M. *et al.* (2022) 'Treasure on the Earth—Gold Nanoparticles and Their Biomedical Applications', *Materials 2022, Vol. 15, Page 3355*. Multidisciplinary Digital Publishing Institute, 15(9), p. 3355. doi: 10.3390/MA15093355.

Naserian, S. *et al.* (2020) 'The TNF/TNFR2 signaling pathway is a key regulatory factor in endothelial progenitor cell immunosuppressive effect', *Cell Communication and Signaling*. BioMed Central Ltd., 18(1), pp. 1–14. doi: 10.1186/S12964-020-00564-3/FIGURES/7.

Oliveira, J. P. *et al.* (2020) 'A helpful method for controlled synthesis of monodisperse gold nanoparticles through response surface modeling', *Arabian Journal of Chemistry*. doi: 10.1016/j.arabjc.2017.04.003.

Palazón, A. *et al.* (2011) 'Agonist anti-CD137 mAb act on tumor endothelial cells to enhance recruitment of activated T lymphocytes', *Cancer research*. Cancer Res, 71(3), pp. 801–811. doi: 10.1158/0008-5472.CAN-10-1733.

Parameswaran, N. and Patial, S. (2010) 'Tumor Necrosis Factor-α Signaling in Macrophages', *Critical reviews in eukaryotic gene expression*. NIH Public Access, 20(2), p. 87. doi: 10.1615/CRITREVEUKARGENEEXPR.V20.I2.10.

Pati, F., Gantelius, J. and Svahn, H. A. (2016) '3D Bioprinting of Tissue/Organ Models', *Angewandte Chemie (International ed. in English)*. Angew Chem Int Ed Engl, 55(15), pp. 4650–4665. doi: 10.1002/ANIE.201505062.

Pobezinskaya, Y. L. and Liu, Z. (2012) 'The role of TRADD in death receptor signaling', *Cell Cycle*. Taylor & Francis, 11(5), p. 871. doi: 10.4161/CC.11.5.19300.

Ridker, Paul M *et al.* (2017) 'Antiinflammatory Therapy with Canakinumab for Atherosclerotic Disease', *New England Journal of Medicine*. Massachusetts Medical Society, 377(12), pp. 1119–1131. doi: 10.1056/NEJMOA1707914/SUPPL_FILE/NEJMOA1707914_DISCLOSURES.PDF.

Ridker, Paul M. *et al.* (2017) 'Effect of interleukin-1β inhibition with canakinumab on incident lung cancer in patients with atherosclerosis: exploratory results from a randomised, double-blind, placebo-controlled trial', *Lancet (London, England)*. Lancet, 390(10105), pp. 1833–1842. doi: 10.1016/S0140-6736(17)32247-X.

Roos, C. *et al.* (2010) 'Soluble and Transmembrane TNF-Like Weak Inducer of Apoptosis Differentially Activate the Classical and Noncanonical NF-κB Pathway', *The Journal of Immunology*. The American Association of Immunologists, 185(3), pp. 1593–1605. doi: 10.4049/jimmunol.0903555.

Saitoh, T. *et al.* (2003) 'TWEAK induces NF-kappaB2 p100 processing and long lasting NF-kappaB activation', *The Journal of biological chemistry*. J Biol Chem, 278(38), pp. 36005–36012. doi: 10.1074/JBC.M304266200.

Salzmann, S. *et al.* (2013) 'Fibroblast growth factor inducible (Fn14)-specific antibodies concomitantly display signaling pathway-specific agonistic and antagonistic activity', *Journal of Biological Chemistry*, 288(19), pp. 13455–13466. doi: 10.1074/jbc.M112.435917.

Schloss, A. C., Williams, D. M. and Regan, L. J. (2016) 'Protein-Based Hydrogels for Tissue Engineering BT - Protein-based Engineered Nanostructures', in Cortajarena, A. L. and Grove, T. Z. (eds). Cham: Springer International Publishing, pp. 167–177. doi: 10.1007/978-3-319-39196-0_8.

Schreiber, R. D., Old, L. J. and Smyth, M. J. (2011) 'Cancer immunoediting: integrating immunity's roles in cancer suppression and promotion', *Science (New York, N.Y.)*. Science, 331(6024), pp. 1565–1570. doi: 10.1126/SCIENCE.1203486.

Scott, A. M., Wolchok, J. D. and Old, L. J. (2012) 'Antibody therapy of cancer', *Nature Reviews Cancer*, 12(4), pp. 278–287. doi: 10.1038/NRC3236.

Sedger, L. M. and McDermott, M. F. (2014) 'TNF and TNF-receptors: From mediators of cell death and inflammation to therapeutic giants - past, present and future', *Cytokine and Growth Factor Reviews*. Elsevier Ltd, 25(4), pp. 453–472. doi: 10.1016/J.CYTOGFR.2014.07.016.

Sessler, T. *et al.* (2013) 'Structural determinants of DISC function: new insights into death receptor-mediated apoptosis signalling', *Pharmacology & therapeutics*. Pharmacol Ther, 140(2), pp. 186–199. doi: 10.1016/J.PHARMTHERA.2013.06.009.

Siegmund, D., Wagner, J. and Wajant, H. (2022) 'TNF Receptor Associated Factor 2 (TRAF2) Signaling in Cancer', *Cancers*. Multidisciplinary Digital Publishing Institute (MDPI), 14(16), p. 4055. doi: 10.3390/CANCERS14164055.

Spranger, S. *et al.* (2017) 'Tumor-residing Batf3 dendritic cells are required for effector T cell trafficking and adoptive T cell therapy', *Cancer cell*. NIH Public Access, 31(5), p. 711. doi: 10.1016/J.CCELL.2017.04.003.

Staros, J. V., Wright, R. W. and Swingle, D. M. (1986) 'Enhancement by N-hydroxysulfosuccinimide of water-soluble carbodiimide-mediated coupling reactions', *Analytical Biochemistry*, 156(1), pp. 220–222. doi: 10.1016/0003-2697(86)90176-4.

Tartaglia, L. A. *et al.* (1993) 'A novel domain within the 55 kd TNF receptor signals cell death', *Cell*, 74(5), pp. 845–853. doi: 10.1016/0092-8674(93)90464-2.

Tsai, E. Y. *et al.* (1996) 'Cell-type-specific regulation of the human tumor necrosis factor alpha gene in B cells and T cells by NFATp and ATF-2/JUN', *Molecular and Cellular Biology*. Informa UK Limited, 16(10), pp. 5232–5244. doi: 10.1128/MCB.16.10.5232.

Turkevich, J., Stevenson, P. C. and Hillier, J. (1951) 'A study of the nucleation and growth processes in the synthesis of colloidal gold', *Discussions of the Faraday Society*, 11, pp. 55–75. doi: 10.1039/DF9511100055.

Vinay, D. S. and Kwon, B. S. (2011) '4-1BB signaling beyond T cells', *Cellular & Molecular Immunology 2011 8:4*. Nature Publishing Group, 8(4), pp. 281–284. doi: 10.1038/cmi.2010.82.

Wajant, H. (2013) 'The TWEAK-Fn14 system as a potential drug target', *British Journal of Pharmacology*, 170(4), pp. 748–764. doi: 10.1111/bph.12337.

Wajant, H. (2015) 'Principles of antibody-mediated TNF receptor activation', *Cell Death and Differentiation*. Nature Publishing Group, 22(11), pp. 1727–1741. doi: 10.1038/cdd.2015.109.

Wajant, H., Henkler, F. and Scheurich, P. (2001) 'The TNF-receptor-associated factor family Scaffold molecules for cytokine receptors , kinases and their regulators', 13.

Wallach, D. *et al.* (1999) 'TUMOR NECROSIS FACTOR RECEPTOR AND Fas SIGNALING MECHANISMS', *Annual Review of Immunology*. Annual Reviews, 17(1), pp. 331–367. doi: 10.1146/annurev.immunol.17.1.331.

Wicovsky, A. *et al.* (2009) 'TNF-like weak inducer of apoptosis inhibits proinflammatory TNF receptor-1 signaling.', *Cell death and differentiation*. England, 16(11), pp. 1445–1459. doi: 10.1038/cdd.2009.80.

Wiley, S. R. *et al.* (2001) 'A novel TNF receptor family member binds TWEAK and is implicated in angiogenesis', *Immunity*. Cell Press, 15(5), pp. 837–846. doi: 10.1016/S1074-7613(01)00232-1.

Willis, A. L. *et al.* (2008) 'The fibroblast growth factor-inducible 14 receptor is highly expressed in HER2-positive breast tumors and regulates breast cancer cell invasive capacity', *Molecular cancer research : MCR*. Mol Cancer Res, 6(5), pp. 725–734. doi: 10.1158/1541-7786.MCR-08-0005.

Winkles, J. A. (2008) 'The TWEAK-Fn14 cytokine-receptor axis: Discovery, biology and therapeutic targeting', *Nature Reviews Drug Discovery*, 7(5), pp. 411–425. doi: 10.1038/nrd2488.

Wyzgol, A. *et al.* (2009) 'Trimer stabilization, oligomerization, and antibody-mediated cell surface immobilization improve the activity of soluble trimers of CD27L, CD40L, 41BBL, and glucocorticoid-induced TNF receptor ligand.', *Journal of immunology (Baltimore, Md. : 1950)*. United States, 183(3), pp. 1851–1861. doi: 10.4049/jimmunol.0802597.

Yan, L., Zheng, D. and Xu, R. H. (2018) 'Critical Role of Tumor Necrosis Factor Signaling in Mesenchymal Stem Cell-Based Therapy for Autoimmune and Inflammatory Diseases', *Frontiers in immunology*. Front Immunol, 9(JUL). doi: 10.3389/FIMMU.2018.01658.

Yang, S. *et al.* (2018) 'Role of TNF-TNF Receptor 2 Signal in Regulatory T Cells and Its Therapeutic Implications', *Frontiers in immunology*. Front Immunol, 9(APR). doi: 10.3389/FIMMU.2018.00784.

You, C.-C., Arvizo, R. R. and Rotello, V. M. (2006) 'Regulation of alpha-chymotrypsin activity on the surface of substrate-functionalized gold nanoparticles.', *Chemical communications (Cambridge, England)*. England, (27), pp. 2905–2907. doi: 10.1039/b605508g.

Zhang, S. *et al.* (2023) 'Convergence of 3D Bioprinting and Nanotechnology in Tissue Engineering Scaffolds', *Biomimetics 2023, Vol. 8, Page 94*. Multidisciplinary Digital Publishing Institute, 8(1), p. 94. doi: 10.3390/BIOMIMETICS8010094.

Zhang, T. *et al.* (2011) 'A new strategy improves assembly efficiency of DNA mono-modified gold nanoparticles.', *Chemical communications (Cambridge, England)*. England, 47(20), pp. 5774–5776. doi: 10.1039/c1cc11337b.

Zhang, X. (2015) 'Gold Nanop[1] X. Zhang, "Gold Nanoparticles: Recent Advances in the Biomedical Applications," Cell Biochem. Biophys., vol. 72, no. 3, pp. 771–775, Jul. 2015.articles: Recent Advances in the Biomedical Applications', *Cell biochemistry and biophysics*. Cell Biochem Biophys, 72(3), pp. 771–775. doi: 10.1007/S12013-015-0529-4.

Zhang, Y. *et al.* (2018) 'Nanoparticle anchoring targets immune agonists to tumors enabling anti-cancer immunity without systemic toxicity', *Nature Communications 2017 9:1*. Nature Publishing Group, 9(1), pp. 1–15. doi: 10.1038/s41467-017-02251-3.

Zhang, Y. S. *et al.* (2016) '3D Bioprinting for Tissue and Organ Fabrication', *Annals of Biomedical Engineering 2016 45:1*. Springer, 45(1), pp. 148–163. doi: 10.1007/S10439-016-1612-8.

# 9. Attachments

## 9.1. List of Figures

## 9.2. List of Tables



## 9.3. List of Publications:

**Anti-Fn14 Antibody-Conjugated Nanoparticles Display Membrane TWEAK-Like Agonism**

Authors: **Ahmed Aido**, Olena Zaitseva, Harald Wajant, Matej Buzgo and Aiva Simaite

Journal: **Pharmaceutics 2021,13, 1072**

## 9.4. Curriculum Vitae